CHAPTER II
LITERATURE REVIEW

2.1 Ionic Liquids

Ionic liquids (ILs) are a new generation of solvents that have been considered as environmentally benign solvents and demonstrated, successfully, as potential replacements for conventional media in chemical processes, especially in reactions and separations (Kim *et al.*, 2005; Zhang *et al.*, 2011). Ionic liquids refer to organic salts entirely composed of ions (Petkovic *et al.*, 2011), which in this sense resemble the ionic melts produced by heating normal metallic salts such as sodium chloride to high temperature (e.g. NaCl to over 800 °C) (Huddleston and Rogers, 1998). Ionic liquids remain liquids in their pure states at ambient conditions (Seddon, 1997). Many refer to any salt with a melting point less than 100 °C as an ionic liquid. Particularly, ionic liquids having melting points at room temperature are usually called "Room Temperature Ionic Liquid (RTIL)". The terms, nonaqueous ionic liquid, molten salt, liquid organic salt and fused salt have been employed to describe ionic liquids as well (Arshad, 2009).

Figure 2.1 shows the ionic configuration of inorganic salts and ionic liquids. The factors which affect the melting point are the charge distribution on the ions, H-bonding ability, the symmetry of the ions, and van der Waals interactions. When compared to typical inorganic salts, ionic liquids have a significantly lower symmetry. The combination of bulky asymmetric organic cations (usually 1-alkyl-3-methylimidazolium, 1-alkylpyridinium, 1-methyl-1-alkylpyrrolidinium or ammonium ions) and inorganic (halides, tetrafluoroborate, hexafluorophosphate and bis(trifluorosulfonyl)imide) or organic anions (triflate, tosylate and alkylsulfate) are not capable of making the resulting salts pack compactly, thus lowering the lattice energy and having low melting points. As a result of noncrystalline salts, ionic liquids can remain liquids through a wide range of temperature. In some cases, the relatively large anions play a crucial role in lowering the melting point (Marsh *et al.*, 2004; Laus *et al.*, 2005; Keskin *et al.*, 2007).

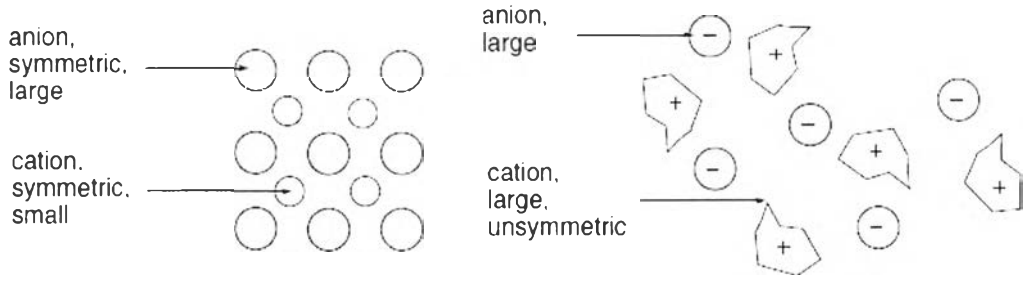

Figure 2.1 Ionic configuration of inorganic salts (left) and ionic liquids (right) (Sigma-Aldrich, US).

Figure 2.2 represents some cations and anions being able to form ionic liquids. Commonly used cations include imidazolium, pyridinium, pyrroridinium, tetra alkylphosphonium, quaternary ammonium and sulfonium based. For anions, tetrafluoroborate (BF_4^-), hexafluorophosphate (PF_6^-), acetate ($CH_3CO_2^-$), trifluoroacetate ($CF_3CO_2^-$), nitrate (NO_3^-), triflate ($CF_3SO_3^-$), bis(trifluoromethylsulfonyl)imide (Tf_2N^-), chloride (Cl^-), bromide (Br^-) and iodide (I^-) have vastly been reported in many publications. The capability of tailoring the size, shape, and functionality of the component cations and anions during the syntheses makes ionic liquids highly flexible. A number of combinations of cations and anions offer many great opportunities to create ionic liquids with specific physicochemical properties for any particular application. One of the most fascinating areas of research has been concerned with the structural design of ionic liquids (Tokuda *et al.*, 2006). Researchers have found that large effects on many properties including melting points, viscosities, densities, as well as gas and liquid solubilities rely on the adjustment of the structure of either cations or anions (Holbrey and Rogers, 2002; Anthony *et al.*, 2003). The choice of cations is generally responsible for the properties and the stability of ionic liquids, which is finely tuned by varying the length and branching of alkyl groups in the cation. On the other hand, the choice of anion has an impact on the chemistry and functionality of ionic liquids. For example, replacing the [PF_6^-] anion of 1-alkyl-3-alkylimidazolium cation with [BF_4^-] anion can dramatically increase the water solubility in the ionic liquid while replacing with the [Tf_2N^-] anion decreases the water solubility (Marsh *et al.*, 2004).

Different combinations of a variety of cations and anions lead to a theoretically feasible number of 10^{18} ionic liquids with unique physicochemical properties but only some of them can be synthesized. At present, approximately 1,000 ionic liquids are described in the literature and about 300 ILs are sold commercially.

Thanks to their unique characteristics, ionic liquids present various advantages over conventional organic solvents. The major advantage which makes them gain interest as green solvents is their negligibly low vapor pressure. This non-volatile property decreases the risk of worker exposure and the loss of solvent to the atmosphere, which is safer than other traditional organic solvents. In addition, ionic liquids are considered as designer solvents due to their tunable properties (Keskin *et al.*, 2007; Hasib-ur-Rahman *et al.*, 2010). The structural tunability such as varying cations, anions and substituents on ionic liquids can tailor for specific applications in order to optimize selectivities, capacities, solubilities and rates of reaction (Brennecke *et al.*, 2008). As designer solvents, choosing the correct ionic liquid can obtain high product yields and produce a reduced amount of waste in a given reaction (Earle and Seddon, 2002).

Nevertheless, an important drawback of some ionic liquids is their high viscosity. Most RTILs are generally viscous liquids whose viscosities are comparable to oils. Their relatively high viscosity, about five folds higher than that of monoethanolamine (MEA), will have an adverse impact on mass transfer and power requirement. During the CO_2 absorption process, higher viscosities of ionic liquids due to an increase in CO_2 loading require additional energy for pumping system. The viscosities can be within an acceptable range by choosing proper cations and anions (Marsh *et al.*, 2004; Keskin *et al.*, 2007; Herzog *et al.*, 2009; Hasib-ur-Rahman *et al.*, 2010).

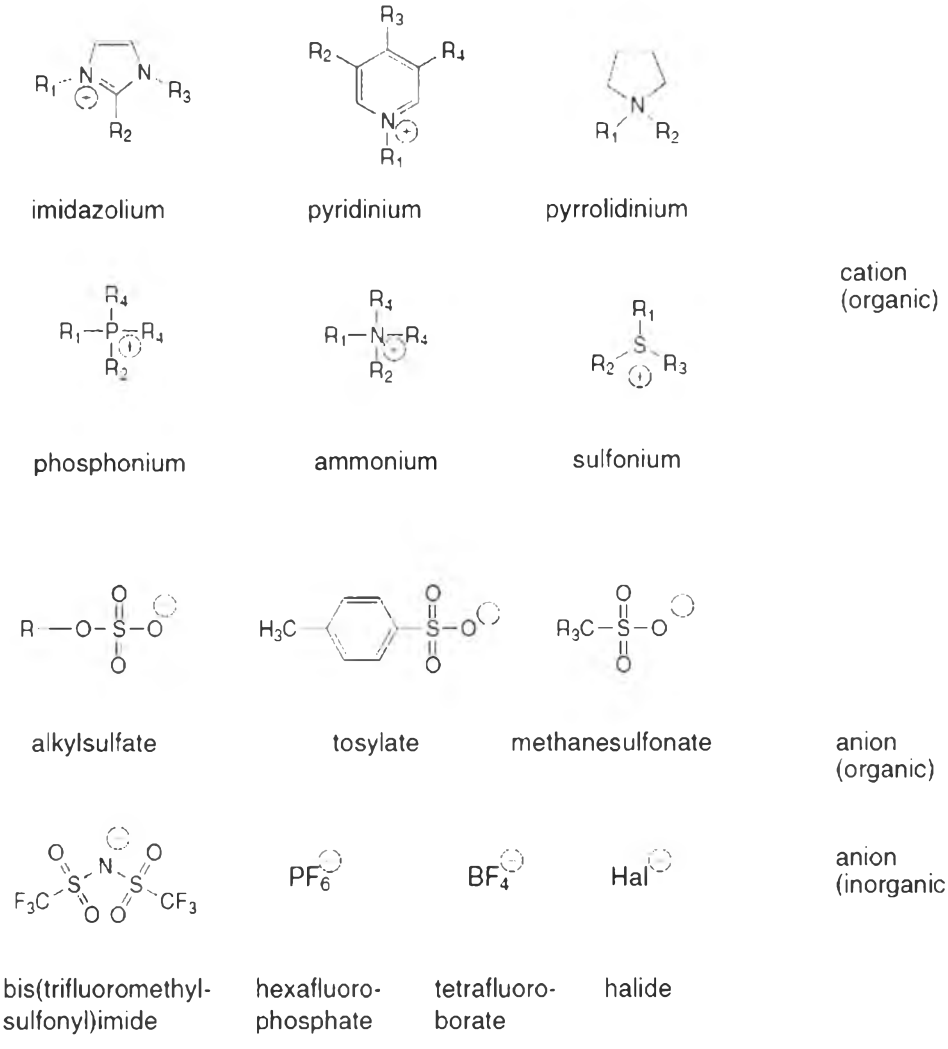

Figure 2.2 Some cations and anions present in ionic liquids (Sigma-Aldrich, US).

2.2 Physical Properties

Ionic liquids have several unique physicochemical properties, which enable them to overcome conventional organic solvents and suit to many specific applications. The properties of ionic liquids are determined by the structure and interaction of ions. For commonly used ionic liquids, they have a wide range of liquid up to about 200 °C, high thermal stability up to about 300 °C, negligible vapor pressure, structural tunability, non-flammability, high thermal conductivity, large electrochemical window, immiscibility with many organic solvents, high CO_2

solubility and recyclability (Marsh *et al.*, 2004; Keskin *et al.*, 2007; Herzog *et al.*, 2009; Hasib-ur-Rahman *et al.*, 2010).

2.2.1 Melting Point

According to the definition, ionic liquids are referred to have melting points below 100 °C and most of them remain in liquid state at room temperature. Both cations and anions influence the melting points of ionic liquids. Low symmetry, weak intermolecular interactions, and a good distribution of charge are outstanding features in the cation of low-melting salts. The large size and the increased asymmetry of the cation result in a melting point reduction. Moreover, the melting point increases as the branching on the alkyl chain increases. In regard to the anion, an increase in the size of the anion leads to a decrease in the melting point of pure ionic liquids (Wasserscheid and Keim, 2000; Mallakpour and Dinari, 2012). Basically, ionic liquids based upon halide anions have higher melting points than those with larger and more complex anions (Domańska *et al.*, 2007). A series of novel hexafluorophosphate salts based on N,N'-dialkylimidazolium and substituted N-alkylpyridinium were studied to explain the liquid crystalline behaviour at temperature above their melting points. It was shown from Figure 2.3 that the melting point of salts increased slightly with increasing alkyl chain length, and the salts based on the pyridinium cation displayed higher melting points than imidazolium salts of equivalent alkyl chain length cations. Furthermore, alkyl substitution at the 3- and 4-positions on the pyridinium ring resulted in a decrease in the melting point compared with the equivalent unsubstituted salt (Gordon *et al.*, 1998). Melting points of some ionic liquids are summarized in Table 2.1.

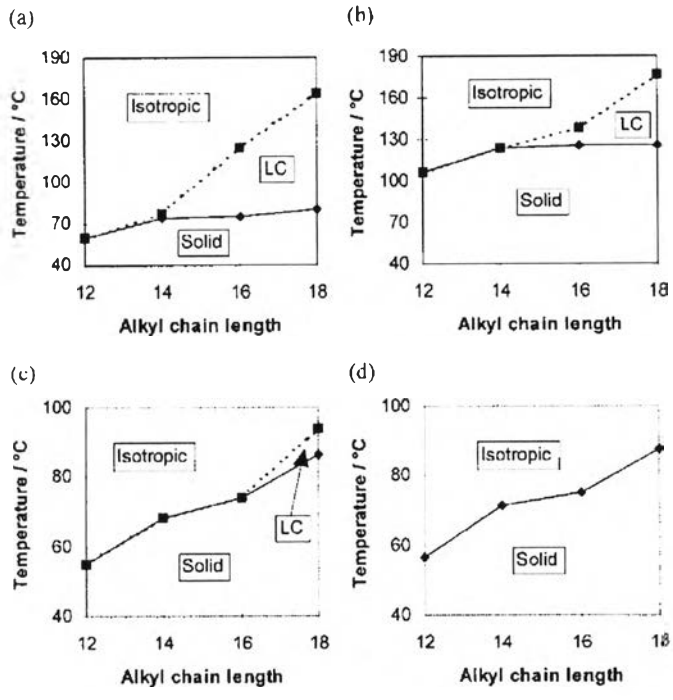

Figure 2.3 Plots showing the melting and clearing temperatures observed on heating of (a) [C_n-mim][PF_6], (b) [C_n-py][PF_6], (c) [C_n-3-Mepy][PF_6], and (d) [C_n-4-Mepy][PF_6] (Gordon *et al.*, 1998).

Table 2.1 Melting points data for several ionic liquids (Huddleston *et al.*, 2001)

Ionic liquids	Melting point (°C)	Ionic liquids	Melting point (°C)
[C_4mim][Cl]	41	[C_2mim][CH_3CO_2]	45
[C_4mim][I]	-72	[C_2mim][PF_6]	58-60
[C_4mim][PF_6]	10	[C_2mim][TfO]	9
[C_1mim][$AlCl_4$]	125	[C_2mim][NfO]	28
[C_2mim][$AlCl_4$]	84	[C_2mim][Tf_2N]	4
[C_3mim][$AlCl_4$]	60	[C_2mim][TA]	14
[C_4mim][$AlCl_4$]	65	[C_3mim][PF_6]	40
[C_4C_4mim][$AlCl_4$]	55	[i-C_3mim][PF_6]	102
[C_2mim][NO_3]	38	[C_4mim][BF_4]	-81
[C_2mim][NO_2]	55	[C_6mim][PF_6]	-61

2.2.2 Density

The densities of ionic liquids are typically higher than the density of water with the values ranging between 1 and 1.6 g/cm^3 (Marsh *et al.*, 2004). Seddon *et al.* (2002) reported the density of 1-alkyl-3-methylimidazolium salts with various anions, [BF_4^-], [PF_6^-], [Cl^-], [$CF_3SO_3^-$] and [NO_3^-]. The density decreases with increasing temperature and longer alkyl chain length. In six ionic liquids, 1-butyl-3-methylimidazolium hexafluorophosphate ([bmim][PF_6]), 1-butyl-3-methyl imidazolium tetrafluoroborate ([bmim][BF_4]), 1-butyl-3-methylimidazolium bis(trifluoromethylsulfonyl)imide ([bmim][Tf_2N]), 1-ethyl-3-methylimidazolium bis(trifluoromethylsulfonyl)imide ([emim][Tf_2N]), 1-ethyl-3-methylimidazolium ethylsulfate ([emim][$EtSO_4$]) and butyltrimethylammonium bis(trifluoromethyl sulfonyl)imide ([N_{4111}][Tf_2N]), the densities were measured as a function of temperature and ranging from 293 K to 393 K (20-120 °C) using a vibrating tube densimeter from Anton Paar. The density decreases linearly with temperature in the temperature range studied (Jacquemin *et al.*, 2006b). Kim *et al.* (2005) calculated the density of the studied [bmim][PF_6], [C_6mim][PF_6], [emim][BF_4], [C_6mim][BF_4]. [emim][Tf_2N] and [C_6mim][Tf_2N] by a group contribution equation of state at the temperatures ranging from 293 to 343 K (20-70 °C). The results suggested that an increase in the temperature and the alkyl chain length of the ionic liquids led to a decrease in the density, as depicted in Figure 2.4. Densities of various ionic liquids at a temperature of 25 °C are listed in Table 2.2.

In general, the densities of ionic liquids depend on the molar masses of the ions. Ionic liquids containing heavy atoms are denser than those containing lighter atoms. For the same cation species, the densities of the ionic liquids with different types of anions can be arranged in this sequence: [Tf_2N^-] > [PF_6^-] > [BF_4^-]. Nevertheless, this is not true for strongly asymmetric cations. The density decreases with increasing the alkyl chain length on the imidazolium cation (Jacquemin *et al.*, 2006b). A correlation with temperature is usually expressed in terms of a linear equation (equation 2.1):

$$\rho\ (g/cm^3) = a + b(T/K - 273.15) \qquad (2.1)$$

where a and b are the correlation parameters.

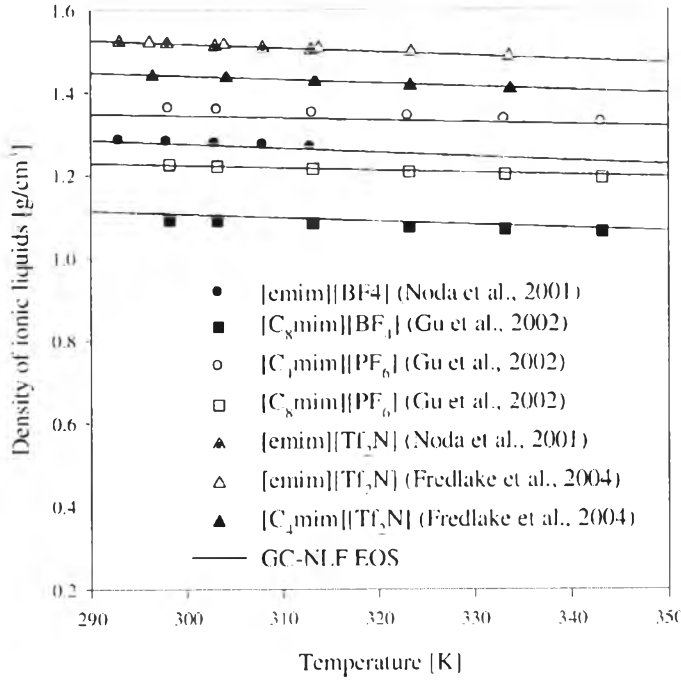

Figure 2.4 Comparison of experimental densities of ionic liquids with calculated values (Kim *et al.*, 2005).

Table 2.2 Densities (25 °C) of several ionic liquids (Huddleston *et al.*, 2001)

Ionic liquids	Density (g/cm^3)
[C_4mim][Cl]	1.08
[C_4mim][I]	1.44
[C_4mim][BF_4]	1.12
[C_4mim][PF_6]	1.36
[C_4mim][Tf_2N]	1.43
[C_6mim][Cl]	1.03
[C_6mim][PF_6]	1.29
[C_8mim][Cl]	1.00
[C_8mim][PF_6]	1.22
[C_4mim][CF_3CO_2]	1.209
[C_4mim][CF_3SO_3]	1.290

2.2.3 Viscosity

Viscosity is one of the most important physical properties of ionic liquids when used as solvents for any process because it influences some practical issues such as stirring and pumping. As known, ionic liquids have relatively high viscosity compared to other common organic solvents. Stirring often might cause a problem in reactions that use ionic liquids as solvents (Tomida *et al.*, 2007). For these reasons, a low viscosity is generally required in order to minimize pumping costs and increase mass transfer rates. For other applications such as lubrication or use in membranes, higher viscosities may be more favorable (Gardas and Coutinho, 2008).

The viscosity of ionic liquids depends on the type of cations and anions. The controlling factors affecting the viscosity of ionic liquids mainly include hydrogen bonding, Van der Waal forces, molecular weight and mobility. With respect to the influence of temperature, the viscosity of ionic liquids decreases significantly with increasing temperature as observed from Figure 2.5. For example, $[C_4mim][PF_6]$ had a viscosity of 270.3 cP at 298.15 K (25 °C), which decreased to 80.4 cP at 323.15 K (50 °C) and 23.5 cP at 353.15 K (70 °C) (Gardas and Coutinho, 2008). Evidently, Figure 2.6 also showed a drastic decrease in the viscosity with increasing temperature (Jacquemin *et al.*, 2006b). For the effect of pressure as presented in Figure 2.7, the viscosity increases as pressure increases; the viscosities of $[C_4mim][PF_6]$, $[C_6mim][PF_6]$, $[C_8mim][BF_4]$, and $[C_8mim][PF_6]$ are more sensitive to pressure than $[C_4mim][BF_4]$ and $[C_4mim][NTf_2]$ (Yu *et al.*, 2012).

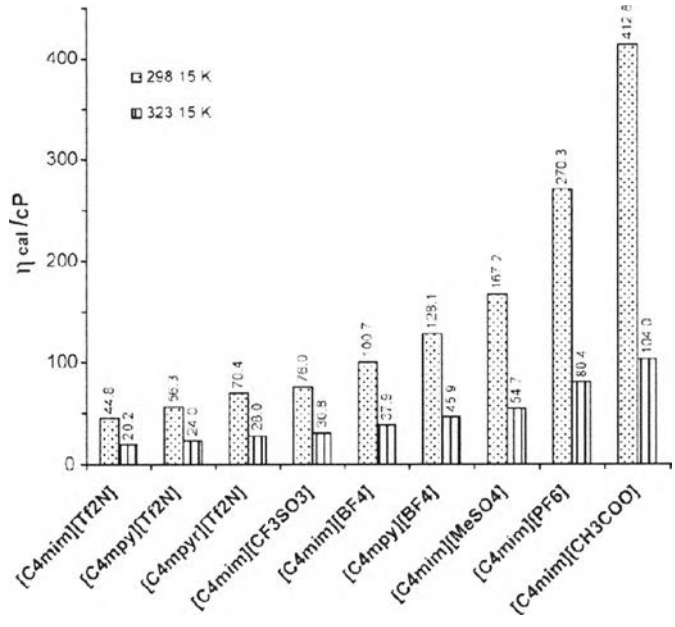

Figure 2.5 Viscosities of imidazolium- and pyridinium-based ionic liquids with butyl chain length and different anions at 298.15 and 323.15 K (25 and 50 °C) (Gardas and Coutinho, 2008).

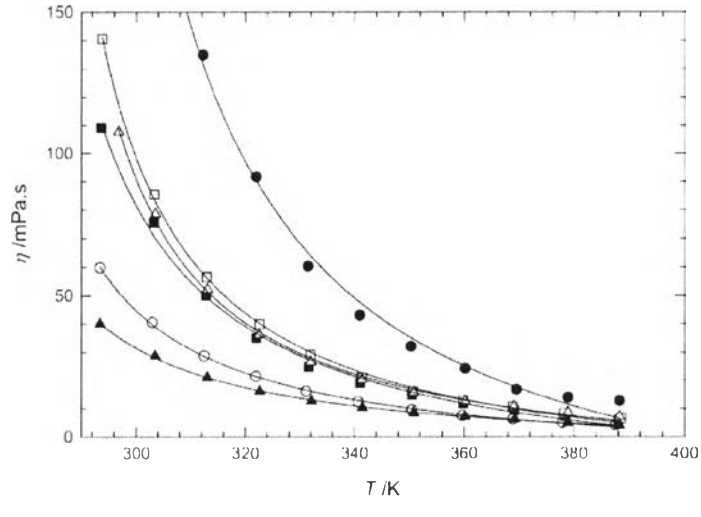

Figure 2.6 Viscosities of ionic liquids as a function of temperature: (●), [bmim][PF_6]; (o), [bmim][Tf_2N]; (■), [bmim][BF_4]; (□), [N_{4111}][Tf_2N]; (▲), [emim][Tf_2N]; (Δ), [emim][$EtSO_4$] (Jacquemin *et al.*, 2006b).

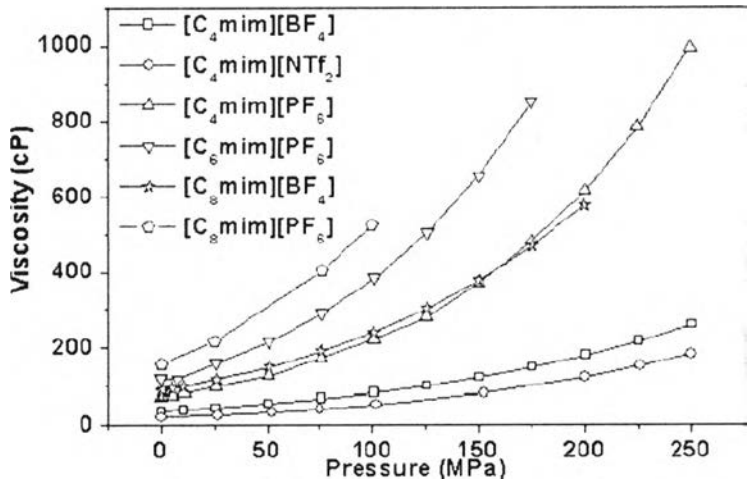

Figure 2.7 Viscosity of ionic liquids as a function of pressure at 323.15 K (50 °C) (Yu *et al.*, 2012).

For ionic liquids paired with the imidazolium cation, the viscosity increased with different anions in the order of $[Tf_2N^-] < [CF_3SO_3^-] < [BF_4^-] < [EtSO_4^-] < [MeSO_4^-] < [PF_6^-] < [CH_3COO^-] < [Cl^-]$. Ionic liquids containing highly symmetric or almost spherical anions are more viscous, whereas those containing less symmetric anions have lower viscosity. For ionic liquids with a similar alkyl chain length on the cation, the viscosity increases with different cations in this sequence: imidazolium ($[Im^+]$) < pyridinium ($[py^+]$) < pyrroridinium ($[pyr^+]$) (Gardas and Coutinho, 2008). It was reported that the alkylammonium-based ionic liquids exhibited a higher viscosity compared to the imidazolium-based ionic liquids with the same anion (Jacquemin *et al.*, 2006b). The effects of characteristic atom/group of cation also influence the viscosity of ionic liquids. All cations with atoms or groups such as –OH, –SR, –COOH, –CBN, and –F will increase the viscosity, except the ionic liquids with alkyl ether, –OR, on cation: they generally have lower viscosity. The fluorination of cation is likely to increase the viscosity as a result of an increase of cationic size and interionic Van der Waals interaction. Meanwhile, the fluorinated anion generally contributes to lower viscosity, resulting from an improved charge distribution and thus the weakness of interionic electrostatic (including possible hydrogen bonding) interaction (Yu *et al.*, 2012). Concerning the effect of the alkyl

chain length, the viscosity increases with an increase in the length of alkyl chain on the cation. For instance, the viscosity at 298.15 K (25 °C) increases monotonously from 172.3 to 677.4 cP in the series of $[C_n mim][PF_6]$ with n from 2 to 8 (Gardas and Coutinho, 2008). It can be described that increasing the length of alkyl side chain will increase van der Waals interaction and thus the viscosity (Yu *et al.*, 2012). The increment of the viscosity with the alkyl chain length of imidazolium cation appears to decrease with the symmetry of anion as the following trend: $[Cl^-] > [CH_3COO^-] > [PF_6^-] > [MeSO_4^-] > [EtSO_4^-] > [BF_4^-] > [CF_3SO_3^-] > [Tf_2N^-]$ (Gardas and Coutinho, 2008).

The common correlation used to express the variation of viscosity with temperature is the Arrhenius law:

$$\eta = \eta_\infty exp(-E_a/RT) \tag{2.2}$$

where viscosity at infinite temperature (η_∞) and the activation energy (E_a) are the characteristic parameters adjusted to fit the experimental data. The Arrhenius law can generally be applied only when the cation presents a limited symmetry. Apart from this case especially in the presence of small and symmetrical cations with low molar mass, the Vogel–Fulcher–Tamman (VFT) equation, an empirical extension of the Arrhenius law, is recommended to correlate the viscosity varying with temperature (Jacquemin *et al.*, 2006b).

$$\eta = AT^{0.5} exp\big(k/(T - T_0)\big) \tag{2.3}$$

where A, k and T_0 are adjustable parameters. Tomida *et al.* (2007) measured the viscosities of 1-hexyl-3-methylimidazolium hexafluorophosphate ($[hmim][PF_6]$) and 1-octyl-3-methylimidazolium hexafluorophosphate ($[omim][PF_6]$) using a rolling ball viscometer at temperatures from 293.15 to 353.15 K (20-80 °C) and pressures up to 20.0 MPa (200 bar). The VTF equation was employed to correlate the experimental viscosites of $[hmim][PF_6]$ and $[omim][PF_6]$ with maximum deviation of 1.2% and 1.6 %, respectively. Harris *et al.* (2007) measured the viscosities of the ionic liquids 1-methyl-3-hexylimidazolium hexafluorophosphate, $[hmim][PF_6]$, and 1-butyl-3-methylimidazolium bis(trifluoromethylsulfonyl)imide, $[bmim][Tf_2N]$, between (0 and 80) °C and at maximum pressures of 238 MPa ($[hmim][PF_6]$) and 300 MPa ($[bmim][Tf_2N]$) at 75 °C with a falling body viscometer. A modified

Vogel-Fulcher-Tammann (VFT) equation was used to represent the temperature and pressure dependence. Besides, other equations, such as the Tait-form equation (Tomida *et al.*, 2007) and the Litovitz equation (Harris *et al.*, 2007), were also used to correlate the experimental data of viscosity. Table 2.3 summarizes viscosities of some ionic liquids.

Table 2.3 Viscosity data (25 °C) for various ionic liquids (Huddleston *et al.*, 2001)

Ionic liquids	Viscosity (cP)
$[C_4mim][I]$	1110
$[C_4mim][BF_4]$	219, 233
$[C_4mim][PF_6]$	450, 312
$[C_4mim][Tf_2N]$	69
$[C_6mim][Cl]$	716
$[C_6mim][PF_6]$	585
$[C_8mim][Cl]$	337
$[C_8mim][PF_6]$	682
$[C_4mim][Tf_2N]$	52
$[C_4mim][CF_3CO_2]$	73
$[C_4mim][CF_3SO_3]$	90
$[C_4mim][CF_3CF_2CF_2CF_2SO_3]$	373
$[C_2mim][BF_4]$	43
$[C_2mim][Tf_2N]$	28

2.2.4 Vapor Pressure

The volatility of ionic liquids is a key property responsible for their escalating popularity. The essentially null volatility enables ionic liquids to be the recognition as environmentally friendly "green" solvents, eventually facilitating their uses in many reactions and separations. This feature makes ionic liquids retain quantitatively in the reaction vessels and separation equipment. Therefore, the environmental impact is minimal (Mallakpour and Dinari, 2012). Owing to green

chemistry concerns and economic reasons, solvents used for chemical processes should be not only "green" but they should also be capable of being recovered for reuse and recycle. Two main problems have been technically faced by researchers: The low vapor pressures of ionic liquids are not measurable at room temperature, whereas some of them may decompose at high temperatures through processes such as the transfer of an alkyl group or through deprotonation in the case of protic ionic liquids. For this reason, commonly used 1-alkyl-3-methylimidazolium bis(trifluoromethylsulfonyl)imide ($[C_nmim][NTf_2]$) with n ranging between 2 and 8 are mostly performed experimentally because of its relatively high thermal stability up to 600 K (Ludwig and Kragl, 2007).

It was hereinbefore believed that ionic liquids exerted negligibly immeasurable vapor pressure and could not be distilled. Nonetheless, Earle *et al.* (2006) reported that many ionic liquids could be distilled at 200-300 °C and low pressure (under vacuum condition) without decomposition using two types of experimental apparatus including the Kugelrohr apparatus (Figure 2.8) and the sublimation apparatus, and they could finally be recondensed at lower temperatures.

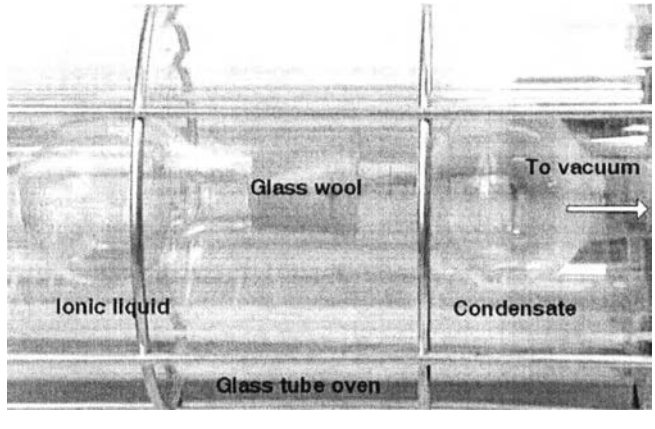

Figure 2.8 The Kugelrohr oven and distillation apparatus (Earle *et al.*, 2006).

In recent years, Taylor *et al.* (2010) investigated the vaporisation of 1-alkyl-3-methylimidazolium bis(trifluoromethylsulfonyl)imide ionic liquids, $[C_nmim][Tf_2N]$ (n = 2, 8), using temperature programmed desorption (TPD) and ultra-high vacuum (UHV) distillation. Ionic liquids have been distilled at UHV and T

> 500 K in a specially designed still. From this perspective, such physicochemical properties including vapor pressures, enthalpies of vaporization and boiling points obviously depend on the cation–anion combination of a given ionic liquid. Adjusting these properties becomes a part of finding the best ionic liquids for any specific application (Ludwig and Kragl, 2007).

2.2.5 Thermal Stability

Another most important factor is the thermal stability of ionic liquids, which also determines the applicability in different separation processes and reactions. Ionic liquids typically have thermal stability up to 450 °C. Most ionic liquids can withstand such high temperatures for a short time. Long time exposure will lead to thermal decomposition eventually. In general, most ionic liquids have negligibly low vapor pressures, suggesting that water can be simply removed by heating under vacuum. Ionic liquids with good thermal stability can be purified to attain water contents below 1 ppm easily (Endres and Zein El Abedin, 2006). Many imidazolium salts are liquids at room temperature and have minimal vapor pressure up to their thermal decomposition temperature (>400 °C), as investigated by thermal gravimetric analyses. Thermal decomposition is found to be endothermic with the inorganic anions and exothermic with the organic anions. Halide anions can drastically reduce the thermal stability of these imidazolium salts below 300 °C. The thermal stability of the imidazolium salts increases with increased alkyl substitution. Moreover, the imidazolium cations are thermally more stable than the tetraalkyl ammonium cations due to the reason that the presence of nitrogen substituted secondary (and likely tertiary) alkyl groups diminishes the thermal stability. The trend of anion stabilities have been suggested in the following order: $[PF_6^-]$ > $[Tf_2N^-]$ ~ $[BF_4^-]$ > halides (Ngo *et al.*, 2000) . Thermal stability data are shown in Table 2.4. The onset of thermal decomposition temperatures is similar for the different cations. The increased cation size from $[C_4mim^+]$ to $[C_8mim^+]$ does not appear to have a profound effect on thermal stability. Even dramatic changes in cation size from $[C_4mim^+]$ to $[C_{18}mim^+]$ still give the same results. However, the thermal decomposition temperatures seem to decrease with an increase in the anion

hydrophilicity (Huddleston *et al.*, 2001). Bonhôte *et al.* (1996) determined the thermal stabilities of $[C_2mim][CF_3SO_3]$ and $[C_2mim][Tf_2N]$ using a thermogravimetric balance. These two ionic liquids exhibited the thermal stability up to 400 °C and decomposed rapidly between 440 and 480 °C. $[C_2mim][TA]$ was much less stable, beginning to decompose at 150 °C and lasting up to 250 °C.

Ionic liquids can alter their colors during thermal decomposition. All of the ionic liquids were investigated to darken from colorless to amber during sonication. The investigations were reported that ionic organic liquids could decompose under ultrasonic conditions. The primary decomposition products for the imidazolium ionic liquids were N-alkylimidazoles and 1-alkylhalides. For instance, during the sonication at 135 °C, 1-butyl-3 methylimidazolium chloride produced the thermal decomposition components such as chlorobutane, chloromethane, and imidazole decomposition products (IDP). 1-butyl-3 methylimidazolium tetrafluoroborate and1-butyl-3-methylimidazolium hexafluorophosphate produced only IDP. The imidazole decomposition products comprise 1,3-butadiene (0.4%), 1,3-butadiyne (2.2%), acetonitrile/isocyanomethane (21.9%), 2-methylpropane (60.7%), 2-propenenitrile (7.4%), pent-3-en-1-yne (7.4%) (Oxley *et al.*, 2003).

Table 2.4 Thermal decomposition temperatures of several ionic liquids (Huddleston *et al.*, 2001)

Ionic liquids	Temperature onset for decomposition (°C)
$[C_4mim][Cl]$	254
$[C_4mim][I]$	265
$[C_4mim][BF_4]$	403
$[C_4mim][PF_6]$	349
$[C_4mim][Tf_2N]$	439
$[C_6mim][Cl]$	253
$[C_6mim][PF_6]$	417
$[C_8mim][Cl]$	243
$[C_8mim][PF_6]$	376
$[C_2mim][Cl]$	285
$[C_2mim][I]$	303
$[C_2mim][PF_6]$	375
$[C_2mim][BF_4]$	412
$[C_2mim][Tf_2N]$	455
$[C_2mim][CF_3COO]$	~150
$[C_2mim][CF_3SO_3]$	~440
$[C_3mim][Cl]$	282
$[C_3mim][PF_6]$	335
$[C_3mim][Tf_2N]$	452
$[C_{18}mim][BF_4]$	360

2.2.6 Surface Tension

Another application of ionic liquids as solvents is to use them in multiphasic homogeneous catalytic reactions, which takes place at the interface between the ionic liquids and the overlying organic phase. The determination of the surface properties of the ionic liquids is required to understand the mechanisms occurring at the interface between two liquids. Measurement of surface tension

therefore plays a crucial role in knowledge of the catalytic mechanisms. Surface tension data for several ionic liquids have been obtained and these are shown in Table 2.5.

Table 2.5 Surface tension data (25 °C) for several ionic liquids (Huddleston *et al.*, 2001)

Ionic liquids	Surface tension (dyn/cm)
$[C_4mim][I]$	54.7
$[C_4mim][BF_4]$	46.6
$[C_4mim][PF_6]$	48.8
$[C_4mim][Tf_2N]$	37.5
$[C_6mim][Cl]$	42.5
$[C_6mim][PF_6]$	43.4
$[C_8mim][Cl]$	33.8
$[C_8mim][PF_6]$	36.5

Several experimental methods can be used to measure the surface tension such as du Noüy ring (Huddleston *et al.*, 2001; Law and Watson, 2001; Freire *et al.*, 2007; Zhang *et al.*, 2007; Klomfar *et al.*, 2009), pendant drop (Jiqin *et al.*, 2007), hanging drop (Pereiro *et al.*, 2007), capillary rise (Ghatee and Zolghadr, 2008), Wilhelmy plate (Klomfar *et al.*, 2009), and spinning drop (Muhammad *et al.*, 2008). Law and Watson (2001) first measured the surface tensions of various 1-alkyl-3-methylimidazolium ionic liquids with different anions using a ring tensiometer. A linear variation of surface tension with temperature can be observed from Figure 2.9. It can be found that the surface tension decreases with increasing the alkyl chain length for $[C_nmim]$ ionic liquids containing the same anion. For alkylimidazolium ionic liquids with the anion $[PF_6^-]$ at temperature of 363 K, the surface tension diminishes from a value of 42.9 mJ/m^2 for [bmim] to 32.8 mJ/m^2 for [omim] to 23.6 mJ/m^2 for $[C_{12}mim]$ as the alkyl chain of the cation increases. A similar variation can be observed for the alkylimidazolium salts with $[BF_4^-]$ as well.

For a fixed cation, ionic liquids containing the larger anion have the higher surface tension at the same temperature. At 336 K, the surface tension of [bmim][PF_6] is higher than that of [bmim][BF_4] and that of [omim][Br] is higher than that of [omim][Cl]. However, It is observed from the figure that [C_{12}mim][PF_6], which has larger anion, exhibits a slightly lower surface tension than [C_{12}mim][BF_4]. Freire *et al.* (2007) concluded that the surface tensions were dependent on the strength of the interactions between the anions and cations, mostly the hydrogen bonds. An increase in the size of the anion led to a decrease on the surface tensions in the following sequence of [BF_4^-] > [PF_6^-] > [$CF_3SO_3^-$] > [Tf_2N^-].

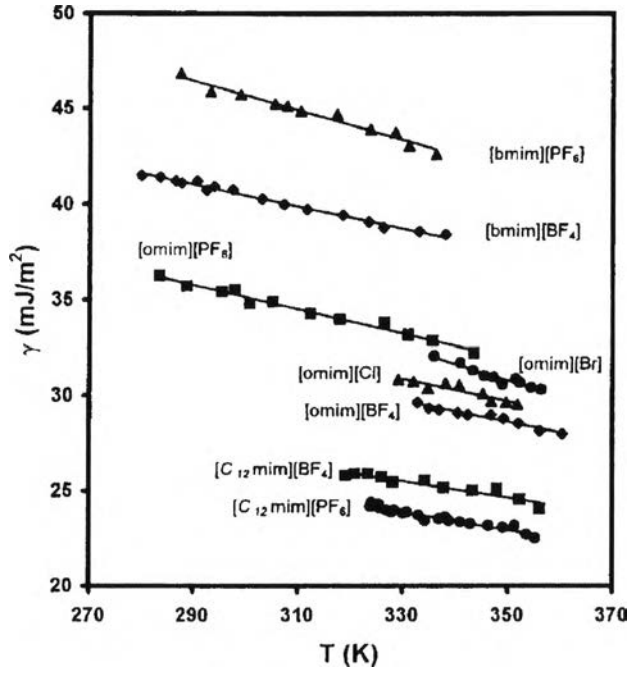

Figure 2.9 Surface tensions (mJ/m^2) of several ionic liquids as a function of temperature (Law and Watson, 2001).

2.2.7 Miscibility with Water

The miscibility of ionic liquids with water depends primarily on the choice of anion as indicated in Figure 2.10. At room temperature, all $[C_nmim][PF_6]$ and $[C_nmim][(CF_3SO_2)_2N]$ ionic liquids are insoluble in water. In particular, 1-alkyl-3-methylimidazolium hexafluorophosphate ionic liquids are commonly regarded as a hydrophobic ionic liquid by many researchers in this field because it forms biphasic systems with water. All halide, ethanoate, nitrate, and trifluoroacetate based ionic liquids are fully water-soluble. However, ionic liquids based on $[BF_4^-]$ and $[CF_3SO_3^-]$ have moderate water miscibility and locate somewhere in between. In addition to the anion's point of view, the water miscibility also relies on the alkyl chain length on the cation, which is a secondary effect. For instance, ionic liquids based on $[BF_4^-]$ are either fully miscible with water (e.g., $[C_2mim][BF_4]$ and $[C_4mim][BF_4]$) or form biphasic systems ($[C_nmim][BF_4]$, $n > 4$) (Seddon *et al.*, 2000). In three ionic liquids: 1-n-butyl-3-methylimidazolium hexafluorophosphate ($[bmim][PF_6]$), 1-n-octyl-3-methylimidazolium hexafluorophosphate ($[C_8mim][PF_6]$), and 1-n-octyl-3-methylimidazolium tetrafluoroborate ($[C_8mim][BF_4]$), the affinity for water was investigated to be greater for ionic liquids with $[BF_4^-]$ anion than those with $[PF_6^-]$, and the water affinity decreased with an increase in the alkyl chain length on the cation (Anthony *et al.*, 2001). Recently, mutual solubilities of 1,500 ionic liquids (50 cations, 30 anions) with water at 25 °C were predicted by using the conductor-like screening model for real solvents (COSMO-RS) as a thermodynamic model, which are very helpful for fast prescreening and for guiding the molecular structure design of ionic liquids. The strong influence of anions on water solubilities was analyzed. With regard to cations, short and monobranched alkyl groups were recommended for enhancing the miscibility of ionic liquids with water (Zhou *et al.*, 2012).

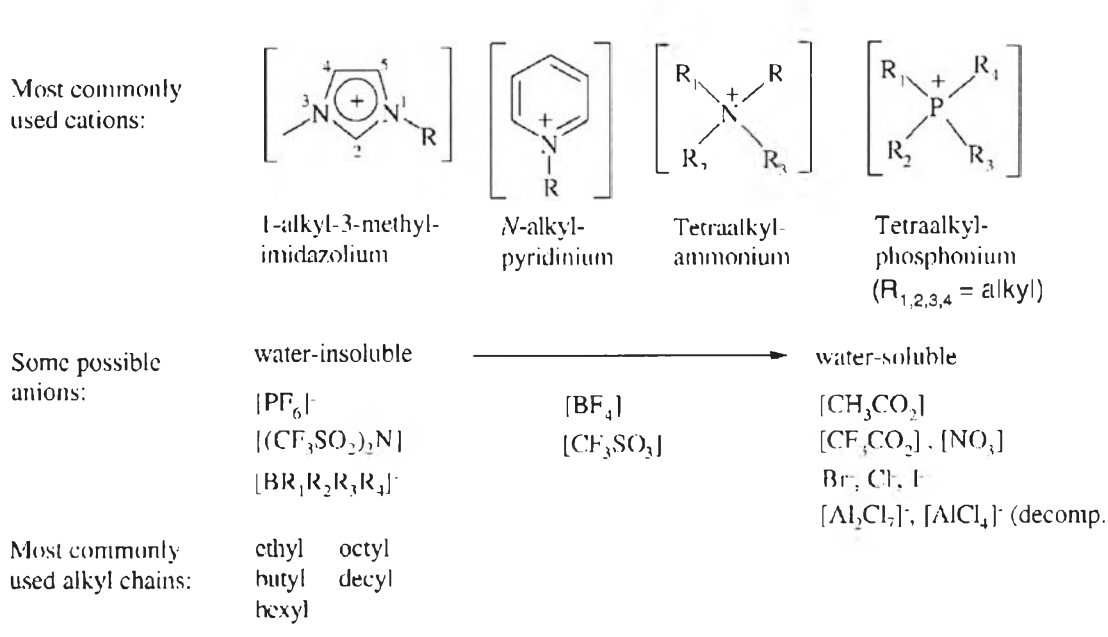

Figure 2.10 Some commonly used ionic liquids and the level of water miscibility (Seddon *et al.*, 2000).

2.3 Uses and Applications

As a result of the properties mentioned above, research areas on ionic liquids are having a rapidly escalating growth. Ionic liquids have become potential candidates in many applications as illustrated in Figure 2.11. Recently, researchers have discovered many applications dealing with ionic liquids such as solvent replacement, purification of gases, homogeneous and heterogeneous catalysis, biological reactions media, and removal of metal ions (Thuy Pham *et al.*, 2010). Currently, research progress on ionic liquids shows that functionalized ionic liquids, supported ionic liquid membranes, polymerized ionic liquid, and the mixtures of ionic liquids with molecular solvents have possible prospects for CO_2 capture. The future research on ionic liquids in this area would be concentrated on three issues. First, the absorption mechanism of CO_2 and ionic liquids should be obviously understood by combining molecular simulation and experimental characteristics. Second, the new ionic liquid with low cost, low viscosity and high absorption capacity with high selectivity should be developed to reduce the energy demand for

regeneration. Third, the transport phenomena which is very important for designing and operating an industrial unit, especially at low pressure and high temperature, should be studied (Zhao *et al.*, 2012).

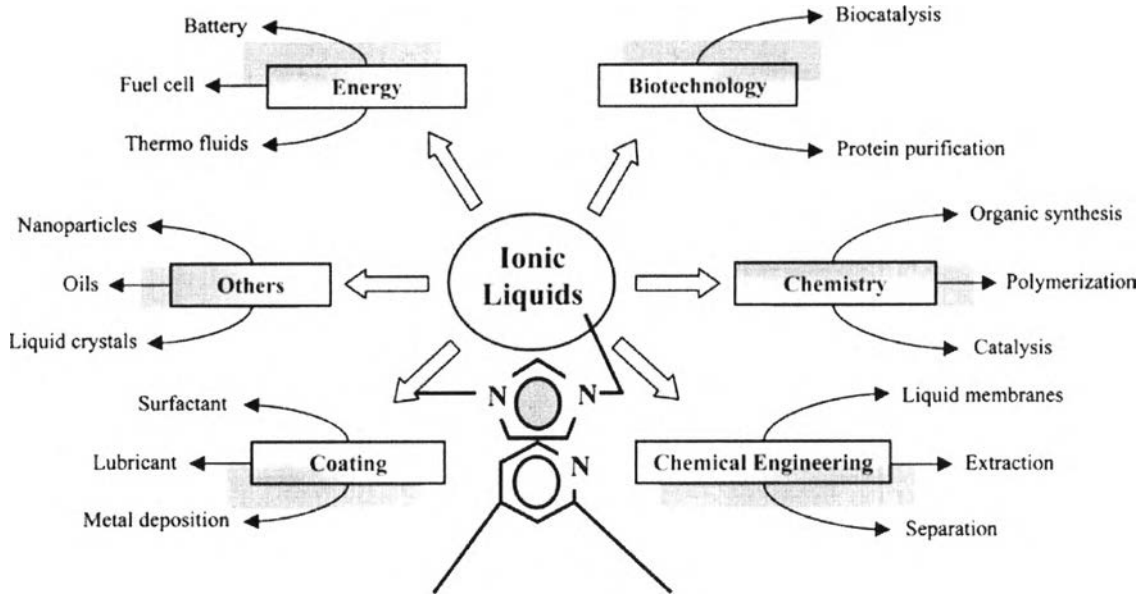

Figure 2.11 Applications of ionic liquids (Thuy Pham *et al.*, 2010).

2.4 Methods for Measuring Gas Solubilities

For gas separation and storage applications, such as the removal of CO_2 from post-combustion flue gas or produced natural gas, knowing gas solubilities can determine the capacities and selectivities. Similarly, the gas solubility in solvents must be known in order to indicate the kinetics when reactions are involved. With the potential uses of ionic liquids in gas separations and reactions, gas solubilities have been extensively studied and measured. Various methods can be used to measure gas solubility in ionic liquids, namely, stoichiometric technique, pressure drop technique and gravimetric methods. Moreover, close cell (static) method, chromatography and several spectroscopic techniques such as Fourier transform infrared spectroscopy (FTIR) are able to determine gas solubility in ionic liquids. Among these techniques,

the most widely used method to measure gas solubility is gravimetric (Brennecke *et al.*, 2008; Soriano *et al.*, 2009b).

2.4.1 Stoichiometric Technique

The concept of this method is to meter known amounts of liquid and gas into a high-pressure viewcell and further determine the gas solubility in that liquid. A simplified schematic of the stoichiometric apparatus is shown in Figure 2.12. The major components of this apparatus are composed of a feed pump, temperature and pressure indicators as well as controllers, a water bath to keep temperature constant, a cathetometer to measure the volume of the liquid in the cell, an optically transparent cell and cell holder, and an agitation system. After loading ionic liquids, adding a known amount of gas into the cell, and leaving the system until thermal equilibrium is reached, the volume of gas remaining in the gas phase is measured, subsequently an accurate equation of state is used to determine the number of moles of gas remaining in the gas phase. Consequently, the amount of gas dissolved in the liquid can be determined by the difference between the known number of moles of gas introduced and the measurable number of moles of gas remaining.

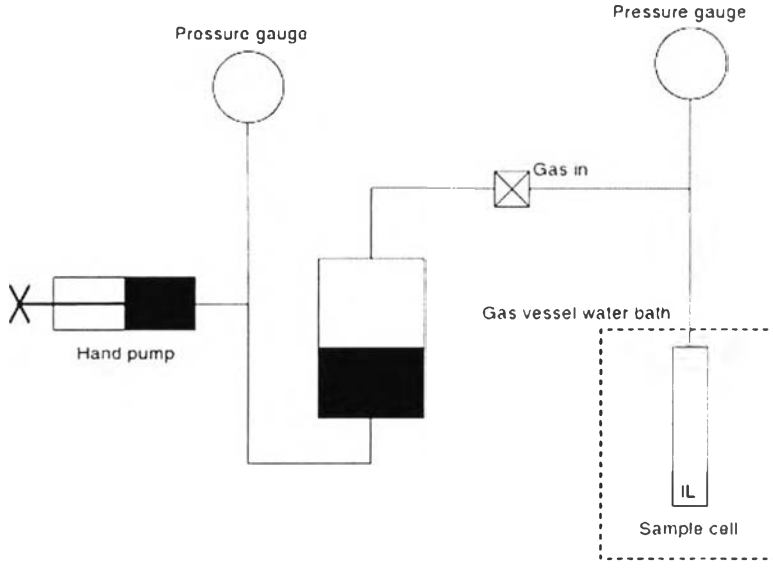

Figure 2.12 The schematic of the stoichiometric apparatus (Brennecke *et al.*, 2008).

In addition to the technique mentioned above, there is another technique for measuring gas solubility by stoichiometric. This technique involves loading known amounts of gas and liquid into the cell and after that increasing the pressure at constant temperature until all the gas dissolves in the liquid. Accordingly, the solubility at various different pressures and pressures can be determined by varying different loadings of the gas (Brennecke *et al.*, 2008).

2.4.2 Pressure Drop Technique

This technique uses the concept of measuring the difference in pressure drop. A known number of moles of gas are stored in a gas vessel and a known amount of ionic liquids is also kept in another liquid vessel. When the valves open, the gas expands and dissolves in the ionic liquid as shown in Figure 2.13. Having reached equilibrium, the measurement of pressure drop will represent the number of moles of gas in the gas phase. The difference between the number of moles of gas in the gas phase and that in the liquid phase can determine the solubility of gas in the ionic liquid (Brennecke *et al.*, 2008).

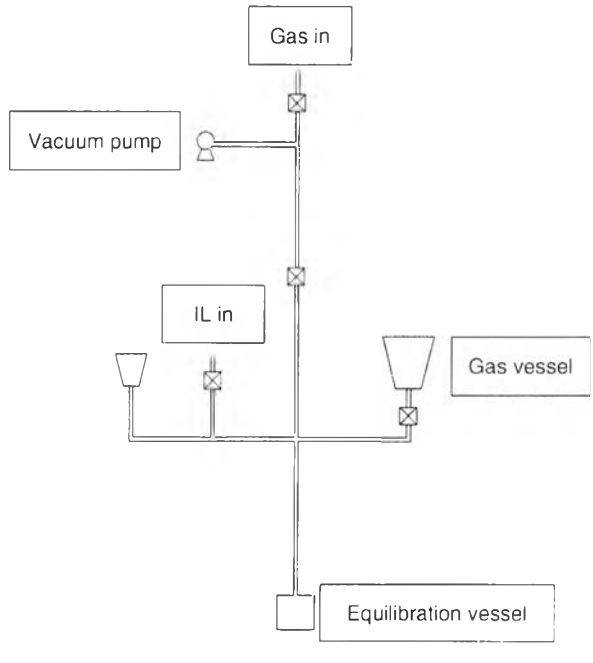

Figure 2.13 The schematic of the pressure drop apparatus (Brennecke *et al.*, 2008).

2.4.3 Gravimetric Methods

The gravimetric method is extensively used and is well suited to determine gas solubilities in ionic liquids due to their unique property (negligible vapor pressure). The gravimetric determination of gas solubility involves feeding the gas through a sample bucket containing the ionic liquid and then weighing the bucket before and after.

Gravimetric microbalances can make the gravimetric measurements more accurate. Figure 2.14 presents the appearance of the Hiden Intelligent Gravimetric Analyzer (IGA003) and Figure 2.15 shows a schematic of the IGA003. The IGA is well-designed to integrate computer control and measurement of mass change, pressure and temperature together, leading to completely automatic and reproducible determination of gas sorption-desorption isotherms and isobars in diverse operating conditions. It can be allowed to operate at a range of temperatures from -196 to 1,000 °C and at pressures ranging from ultra-high vacuum to 20 bar. The microbalance is, in general, composed of a sample bucket and counter weight designed symmetrically so as to minimize buoyancy effects. In an experiment, a small amount of 65-75 mg of ionic liquid samples can be used since the balance has a 1 μg stable resolution. The sample should be predried *in-situ* by evacuating the chamber to 10^{-9} bar and heating it to approximately 70-75 °C in order to get rid of contaminants. Afterwards, the weight of the sample is now stabilized and the gas is fed into the chamber at a specified pressure as well as the set point temperature. While the ionic liquid is absorbing the gas, the weight is monitored as a function of time. The weight change is observed until equilibrium is reached. This process will be further iterative through a set of pressures until the maximum set pressure is attained.

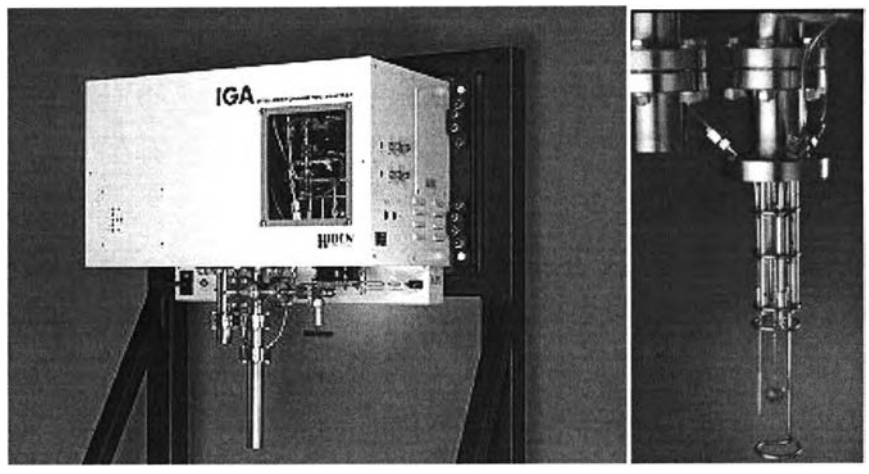

Figure 2.14 The IGA003 gravimetric analyzer (Hiden Analytical Limited, England).

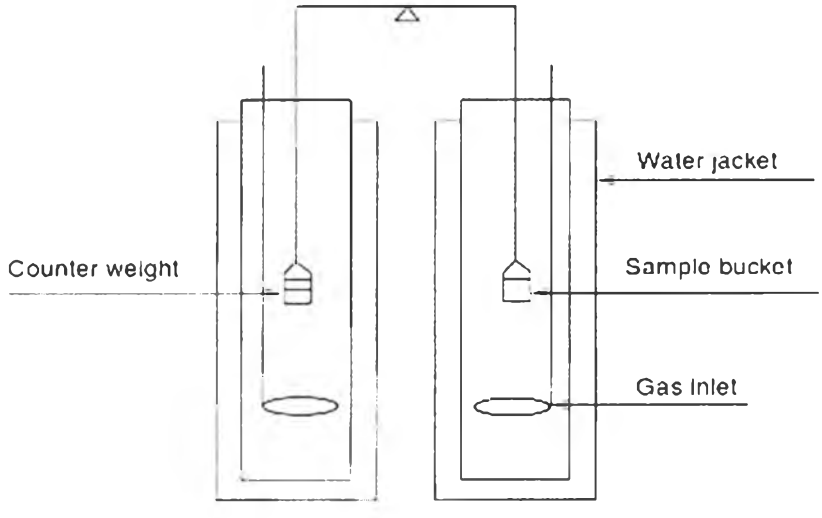

Figure 2.15 The schematic of the intelligent gravimetric analyzer (Brennecke *et al.*, 2008)

However, there are two major concerns in performing experiments by using a gravimetric microbalance. First, buoyancy effects must be taken into consideration even if a symmetric balance is used. Second, the CO_2-IL system should have enough time to reach equilibrium due to the fact that the microbalance does not have any stirring system, depending merely on the diffusion of gas into the ionic

liquid. If the sample is relatively viscous, it will take very long time to achieve equilibrium.

Moreover, there are other apparatuses capable of determining gas solubility in ionic liquids by a gravimetric method. The Rubotherm magnetic suspension balance (Rubotherm, Germany) works on the same principle but can be operated up to 500 bar. The balance which is magnetically coupled to the sorption chamber and not contacted by the gas allows investigation of more toxic and corrosive gases, such as SO_2. Another balance is a quartz crystal microbalance which is based on the principle of the piezoelectric effect. Figures 2.16 and 2.17 present the schematics of Rubotherm magnetically coupled microbalance (Rubotherm, Germany) and quartz crystal microbalance apparatus, respectively (Brennecke *et al.*, 2008).

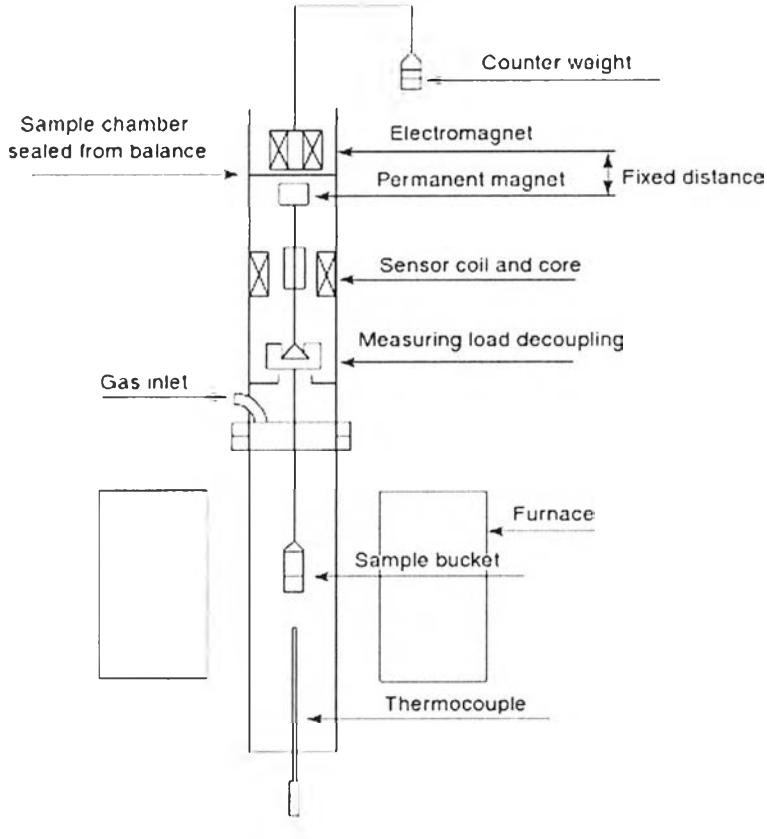

Figure 2.16 The schematic of Rubotherm magnetically coupled microbalance (Brennecke *et al.*, 2008).

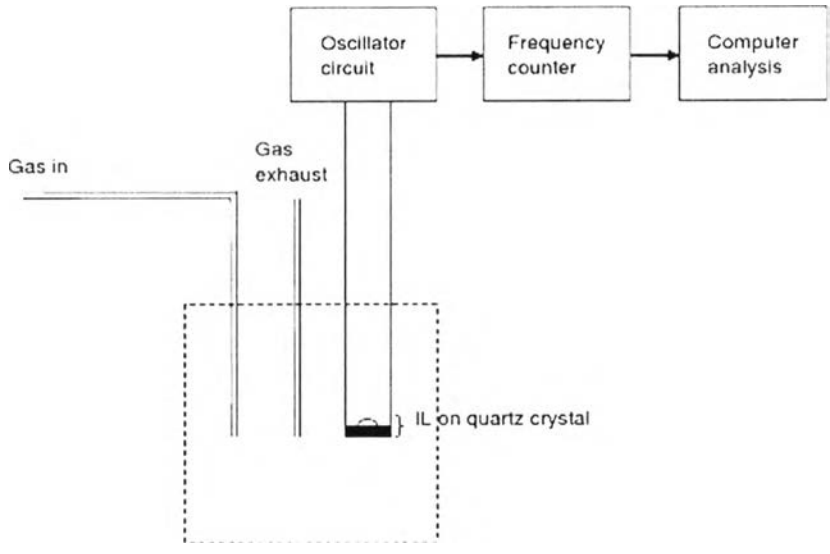

Figure 2.17 The schematic of quartz crystal microbalance apparatus (Brennecke *et al.*, 2008)

2.5 Classification of Ionic Liquids for CO_2 Capture

A number of experimental studies on gas separation process using ionic liquids have been conducted by researchers and are available in the literature. Various investigations have shown that CO_2 is significantly soluble in ionic liquids. In accordance with the structural characteristics and absorption mechanism, ionic liquids can be generally classified into two categories; conventional ionic liquids (second generation) and task-specific ionic liquids (third generation) (Bates *et al.*, 2002). Usually, conventional ionic liquids can absorb less amount of CO_2 because of the physical CO_2-IL interactions. On the other hand, task-specific ionic liquids with alkaline groups can capture greater amount of CO_2 than conventional ones because the chemical interactions or reactivities between CO_2 and ionic liquids are present. This work will concentrate on the solubility of CO_2 in conventional ionic liquids, which will be discussed in the next section in detail.

2.6 CO_2 Solubility in Conventional Ionic Liquids

The gaseous solubility in any solvent plays a crucial role in solvent selection for CO_2 capture. Ionic liquids are, in general, physical solvents displaying the feasibility to be utilized for capturing CO_2. Research on solubilities of CO_2 in ionic liquids has been burgeoning in recent years. Among the ionic liquids investigated, methylimidazolium-based ionic liquids are favorable species for investigation because of their air and water stability, their wide liquids range, the fact that they remain liquid at room temperature, and their relatively favorable viscosity and density characteristics (Huddleston and Rogers, 1998).

Blanchard *et al.* (1999) firstly reported that CO_2 was highly soluble in 1-butyl-3-methylimidazolium hexafluorophosphate ([bmim][PF_6]), reaching a mole fraction of 0.6 at 8 MPa (80 bar) as shown in Figure 2.18. Meanwhile, the solubility of [bmim][PF_6] in CO_2 was less than 10^{-5} mole fraction at 13.8 MPa (138 bar) and 40 °C, indicating the composition of CO_2-rich phase was essentially pure CO_2. Among the six ionic liquids tested, large quantities of CO_2 was found to dissolve in the ionic liquid phase, but no appreciable amount of ionic liquid solubilized in the CO_2 phase (Blanchard *et al.*, 2001). Since an unexpectedly large solubility of CO_2 in ionic liquids and the strongest CO_2-IL interactions compared to other gases such as C_2H_4, C_2H_6, CH_4, Ar, O_2, CO, H_2, and N_2 were observed, an interest in development to explore and understand the solubility of diverse gases in ionic liquids has been growing significantly during the past ten years (Anthony *et al.*, 2002; Herzog *et al.*, 2009). The literature surveys for the solubility of CO_2 in numerous ionic liquids are summarized in Table 2.6.

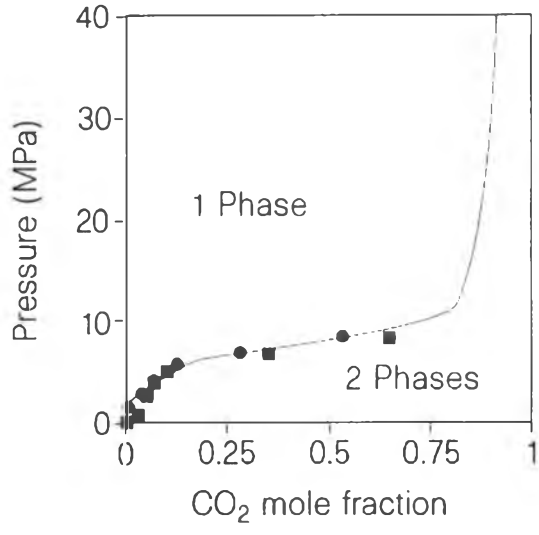

Figure 2.18 CO_2 solubility in [bmim][PF6] at 25 °C (Blanchard *et al.*, 1999).

According to literature surveys, the solubility data of CO_2 in imidazolium based ionic liquids are the most widely reported. Soriano *et al.* (2009b) categorized research on CO_2 solubility of imidazolium based ionic liquids into three groups: (1) low pressure (below 10 bar), (2) moderate pressure (10-70 bar), and (3) high pressure (above 70 bar) (Soriano et al., 2009). For low pressure research, Husson-Borg *et al.* (2003) reported the solubility of CO_2 and O_2 in a commonly used 1-butyl-3-methylimidazolium tetrafluoroborate ([bmim][BF_4]) as a function of temperature ranging from 303.15 K to 343.15 K (30-70 °C) and at pressures ranging from 0.015 MPa to 0.1 MPa (0.15-1.0 bar). The experimental approach was based on an isochoric saturation method. It was observed that CO_2 was one order of magnitude more soluble in the ionic liquid than O_2. Kim *et al.* (2005) experimentally studied the solubility of CO_2 in [bmim][PF_6], [C_6mim][PF_6], [emim][BF_4], [C_6mim][BF_4], [emim][Tf_2N] and [C_6mim][Tf_2N] at 298.15K (25 °C) and up to 1 MPa (10 bar). Kim *et al.* (2007) measured the solubilities of pure CO_2 and propane and those of the mixed gases CO_2 + N_2 and CO_2 + propane in 1-hexyl-3-methylimidazolium bis(trifluoromethylsulfonyl)imide ([C_6mim][Tf_2N]), at 298.15 K (25 °C) and up to 1 MPa (10 bar). They applied the group contribution non-random lattice fluid equation

of state (GC-NLF EoS) to fit the experimental data and the results of both studies were in good agreement. Mostly, research on the CO_2 solubility in ionic liquids containing the imidazolium cation has been extensively investigated at moderate pressures. Kim *et al.* (2011) measured the solubility of CO_2 in 1-butyl-3-methylimidazolium hexafluorophosphate ($[C_4mim][PF_6]$) and 1-nonyl-3-methylimidazolium hexafluorophosphate ($[C_9mim][PF_6]$) at temperatures of 293.15 and 298.15 K (20 and 25 °C) and pressure up to 4 MPa (40 bar) using a stoichiometric phase equilibrium apparatus. The measured data were well correlated using GC-NLF EoS in the low pressure region. Nevertheless, the group parameters of GC-NLF EoS were slightly modified for better prediction at higher pressure and longer alkyl chain.

Table 2.6 Literature surveys for the solubility of CO_2 in numerous ionic liquids

Ionic liquids	T (°C)	P (bar)	Method	Reference
Imidazolium based ionic liquids				
[bmim][PF_6]	20, 25	40	stoichiometric	Kim *et al.* (2011)
	25	10	equilibrium cell	Kim *et al.* (2005)
	10, 25, 50, 75	20	gravimetric microbalance	Shiflett and Yokozeki (2005)
	30	close to atm	surface tension	Kilaru *et al.* (2008)
	10, 25, 50	13	gravimetric microbalance	Anthony *et al.* (2005)
	40, 50, 60	320	high-pressure view cell	Lim *et al.* (2009)
	25 to 60	20	gravimetric microbalance	Galán Sánchez (2008)
	40, 50, 60	95	static high-pressure phase equilibrium	Blanchard *et al.* (2001)
	25, 40, 60	150	stoichiometric	Aki *et al.* (2004)
	24 to 55	0 to 110	high-pressure cell	Zhang *et al.* (2005)
	30	1.07 to 1.20	-	Camper *et al.* (2004)
	40	1.07 to 1.20	-	Camper *et al.* (2005)
	10, 25, 50	13	gravimetric microbalance	Anthony *et al.* (2002)
	10, 25, 50	13	gravimetric microbalance	Cadena *et al.* (2004)
	20 to 140	100	high-pressure view cell	Kumełan *et al.* (2006b)
[bmmim][PF_6]	10, 25, 50	13	gravimetric microbalance	Cadena *et al.* (2004)
[hmim][PF_6]	25	10	equilibrium cell	Kim *et al.* (2005)
	10, 25, 40, 60	up to 13, 13 to 100	gravimetric microbalance, stoichiometric	Muldoon *et al.* (2007)
[omim][PF_6]	40, 50, 60	95	static high-pressure phase equilibrium	Blanchard *et al.* (2001)
[C_9mim][PF_6]	20, 25	40	stoichiometric	Kim *et al.* (2011)
[emim][BF_4]	25	10	equilibrium cell	Kim *et al.* (2005)
	60	-	pressure drop	Blath *et al.* (2011)

Table 2.6 Literature surveys for the solubility of CO_2 in numerous ionic liquids (cont.)

Ionic liquids	T (°C)	P (bar)	Method	Reference
[bmim][BF_4]	60	-	pressure drop	Blath *et al.* (2011)
	10, 25, 50, 75	20	gravimetric microbalance	Shiflett and Yokozeki (2005)
	10, 25, 50	13	gravimetric microbalance	Anthony *et al.* (2005)
	40, 50, 60	320	high-pressure view cell	Lim *et al.* (2009)
	25 to 60	20	gravimetric microbalance	Galán Sánchez (2008)
	25, 40, 60	150	stoichiometric	Aki *et al.* (2004)
	10 to 70	close to atm	isochoric saturation	Jacquemin *et al.* (2006a)
	40	1.07 to 1.20	-	Camper *et al.* (2005)
	10, 25, 50	13	gravimetric microbalance	Cadena *et al.* (2004)
	30 to 70	close to atm	isochoric saturation	Husson-Borg *et al.* (2003)
	32 to 52	10 to 90	high-pressure stainless steel cell	Chen *et al.* (2006)
	up to 100	300	high-pressure variable-volume visual cell	Revelli *et al.* (2010)
[bmmim][BF_4]	10, 25, 50	13	gravimetric microbalance	Cadena *et al.* (2004)
[hmim][BF_4]	25	10	equilibrium cell	Kim *et al.* (2005)
	32 to 52	10 to 90	high-pressure stainless steel cell	Chen *et al.* (2006)
[omim][BF_4]	40, 50, 60	320	high-pressure view cell	Lim *et al.* (2009)
	25 to 60	20	gravimetric microbalance	Galán Sánchez (2008)
	40, 50, 60	95	static high-pressure phase equilibrium	Blanchard *et al.* (2001)
	32 to 52	10 to 90	high-pressure stainless steel cell	Chen *et al.* (2006)
[hemim][BF_4]	30 to 80	11	equilibrium cell	Shokouhi *et al.* (2009)

Table 2.6 Literature surveys for the solubility of CO_2 in numerous ionic liquids (cont.)

Ionic liquids	T (°C)	P (bar)	Method	Reference
[emim][Tf_2N]	25	10	equilibrium cell	Kim *et al.* (2005)
	60	-	pressure drop	Blath *et al.* (2011)
	30	close to atm	surface tension	Kilaru *et al.* (2008)
	30 to 70	close to atm	isochoric saturation	Hong *et al.* (2007)
	37 to 177	0 to 150	Cailletet set-up	Schilderman *et al.* (2007)
	25 to 60	20	gravimetric microbalance	Galán Sánchez (2008)
	10 to 70	close to atm	isochoric saturation	Jacquemin *et al.* (2007)
	30	1.07 to 1.20	-	Camper *et al.* (2004)
	40	1.07 to 1.20	-	Camper *et al.* (2005)
	10, 25, 50	13	gravimetric microbalance	Cadena *et al.* (2004)
[emmim][Tf_2N]	10, 25, 50	13	gravimetric microbalance	Cadena *et al.* (2004)
[bmim][Tf_2N]	10, 25, 50	13	gravimetric microbalance	Anthony *et al.* (2005)
	10 to 70	close to atm	isochoric saturation	Jacquemin *et al.* (2007)
	40, 50	80 to 220	isochoric saturation	Manic *et al.* (2012)
	25, 40, 60	150	stoichiometric	Aki *et al.* (2004)
	10, 25, 40, 60	up to 13, 13 to 100	gravimetric microbalance, stoichiometric	Muldoon *et al.* (2007)
[hmim][Tf_2N]	25	10	equilibrium cell	Kim *et al.* (2005)
	60	-	pressure drop	Blath *et al.* (2011)
	9, 24, 50, 75	20	gravimetric microbalance	Shiflett and Yokozeki (2007)
	25, 40, 60	150	stoichiometric	Aki *et al.* (2004)
	10, 25, 40, 60	up to 13, 13 to 100	gravimetric microbalance, stoichiometric	Muldoon *et al.* (2007)

Table 2.6 Literature surveys for the solubility of CO_2 in numerous ionic liquids (cont.)

Ionic liquids	T (°C)	P (bar)	Method	Reference
[hmmim][Tf_2N]	25, 40, 60	150	stoichiometric	Aki *et al.* (2004)
	10, 25, 40, 60	up to 13, 13 to 100	gravimetric microbalance, stoichiometric	Muldoon *et al.* (2007)
[omim][Tf_2N]	25, 40, 60	150	stoichiometric	Aki *et al.* (2004)
[C_{10}mim][Tf_2N]	40, 50	80 to 220	isochoric saturation	Manic *et al.* (2012)
[emim][TfO]	60	-	pressure drop	Blath *et al.* (2011)
	30	close to atm	surface tension	Kilaru *et al.* (2008)
	30 to 70	59	thermogravimetric microbalance	Soriano *et al.* (2009a)
	30.7 to 71.4	400	volume cell	Shin and Lee (2008)
	30	1.07 to 1.20	-	Camper *et al.* (2004)
	40	1.07 to 1.20	-	Camper *et al.* (2005)
[bmim][TfO]	30 to 70	65	thermogravimetric microbalance	Soriano *et al.* (2009b)
	30.7 to 71.4	400	volume cell	Shin and Lee (2008)
	25, 40, 60	150	stoichiometric	Aki *et al.* (2004)
[hmim][TfO]	30.7 to 71.4	400	volume cell	Shin and Lee (2008)
[omim][TfO]	30.7 to 71.4	400	volume cell	Shin and Lee (2008)
[desmim][TfO]	30	close to atm	surface tension	Kilaru *et al.* (2008)
[emim][$EtSO_4$]	30 to 70	65	thermogravimetric microbalance	Soriano *et al.* (2009b)
	10 to 70	close to atm	isochoric saturation	Jacquemin *et al.* (2008)
	40, 50, 60	95	static high-pressure phase equilibrium	Blanchard *et al.* (2001)
[emim][DCA]	30 to 70	65	thermogravimetric microbalance	Soriano *et al.* (2009b)
	30	1.07 to 1.20	-	Camper *et al.* (2004)
	40	1.07 to 1.20	-	Camper *et al.* (2005)

Table 2.6 Literature surveys for the solubility of CO_2 in numerous ionic liquids (cont.)

Ionic liquids	T (°C)	P (bar)	Method	Reference
[bmim][DCA]	25 to 60	20	gravimetric microbalance	Galán Sánchez (2008)
	25, 40, 60	150	stoichiometric	Aki *et al.* (2004)
[bmim][$B(CN)_4$]	60	-	pressure drop	Blath *et al.* (2011)
[hmim][eFAP]	60	-	pressure drop	Blath *et al.* (2011)
	10, 25, 40, 60	up to 13, 13 to 100	gravimetric microbalance, stoichiometric	Muldoon *et al.* (2007)
	10, 25, 50	18	gravimetric microbalance	Zhang *et al.* (2008)
[hmim][pFAP]	10, 25, 40, 60	up to 13, 13 to 100	gravimetric microbalance, stoichiometric	Muldoon *et al.* (2007)
[C_5mim][bFAP]	10, 25, 40, 60	up to 13, 13 to 100	gravimetric microbalance, stoichiometric	Muldoon *et al.* (2007)
[bmim][SCN]	25 to 60	20	gravimetric microbalance	Galán Sánchez (2008)
	up to 100	300	high-pressure variable-volume visual cell	Revelli *et al.* (2010)
[bmim][$MeSO_4$]	25 to 60	20	gravimetric microbalance	Galán Sánchez (2008)
	20 to 140	100	high-pressure view cell	Kumełan *et al.* (2006b)
[bmim][C_8SO_4]	10 to 70	close to atm	isochoric saturation	Jacquemin *et al.* (2008)
[dmim][Me_2PO_4]	40 to 60	close to atm	isochoric saturation	Palgunadi *et al.* (2009)
	up to 100	300	high-pressure variable-volume visual cell	Revelli *et al.* (2010)
[emim][Et_2PO_4]	40 to 60	close to atm	isochoric saturation	Palgunadi *et al.* (2009)
[bmim][Bu_2PO_4]	40 to 60	close to atm	isochoric saturation	Palgunadi *et al.* (2009)
[bmim][NO_3]	40, 50, 60	95	static high-pressure phase equilibrium	Blanchard *et al.* (2001)
	25, 40, 60	150	stoichiometric	Aki *et al.* (2004)

Table 2.6 Literature surveys for the solubility of CO_2 in numerous ionic liquids (cont.)

Ionic liquids	T (°C)	P (bar)	Method	Reference
[emim][Ac]	25, 50, 75	20	gravimetric microbalance	Shiflett and Yokozeki (2009)
[bmim][Ac]	10, 25, 50, 75	20	gravimetric microbalance	Shiflett *et al.* (2008)
	10, 25, 40, 60	up to 13, 13 to 100	gravimetric microbalance, stoichiometric	Muldoon *et al.* (2007)
[emim][TfAc]	25, 50, 75	20	gravimetric microbalance	Shiflett and Yokozeki (2009)
[bmim][methide]	25, 40, 60	150	stoichiometric	Aki *et al.* (2004)
	10, 25, 40, 60	up to 13, 13 to 100	gravimetric microbalance, stoichiometric	Muldoon *et al.* (2007)
[bmim][$C_7F_{15}CO_2$]	10, 25, 40, 60	up to 13, 13 to 100	gravimetric microbalance, stoichiometric	Muldoon *et al.* (2007)
[$C_6H_4F_9$mim][Tf_2N]	10, 25, 40, 60	up to 13, 13 to 100	gravimetric microbalance, stoichiometric	Muldoon *et al.* (2007)
[$C_8H_4F_{13}$mim][Tf_2N]	10, 25, 40, 60	up to 13, 13 to 100	gravimetric microbalance, stoichiometric	Muldoon *et al.* (2007)
[hmim][SAC]	10, 25, 40, 60	up to 13, 13 to 100	gravimetric microbalance, stoichiometric	Muldoon *et al.* (2007)
[hmim][ACE]	10, 25, 40, 60	up to 13, 13 to 100	gravimetric microbalance, stoichiometric	Muldoon *et al.* (2007)
[Et_3NBH_2mim][Tf_2N]	10, 25, 40, 60	up to 13, 13 to 100	gravimetric microbalance, stoichiometric	Muldoon *et al.* (2007)
[$(ETO)_2$im][Tf_2N]	up to 100	300	high-pressure variable-volume visual cell	Revelli *et al.* (2010)
Pyridinium based ionic liquids				
[MeBuPy][BF_4]	25 to 60	20	gravimetric microbalance	Galán Sánchez (2008)
[N-bupy][BF_4]	40, 50, 60	95	static high-pressure phase equilibrium	Blanchard *et al.* (2001)

Table 2.6 Literature surveys for the solubility of CO_2 in numerous ionic liquids (cont.)

Ionic liquids	T (°C)	P (bar)	Method	Reference
$[C_4py][Tf_2N]$	25, 40, 60	0.25 to 10	magnetic suspension balance	Yunus *et al.* (2012)
[BM-Pyrrolid][Tf_2N]	60	-	pressure drop	Blath *et al.* (2011)
[hmpy][Tf_2N]	10, 25, 40, 60	up to 13, 13 to 100	gravimetric microbalance, stoichiometric	Muldoon *et al.* (2007)
[H-pyrid][Tf_2N]	60	-	pressure drop	Blath *et al.* (2011)
$[C_8py][Tf_2N]$	25, 40, 60	0.25 to 10	magnetic suspension balance	Yunus *et al.* (2012)
$[C_{10}py][Tf_2N]$	25, 40, 60	0.25 to 10	magnetic suspension balance	Yunus *et al.* (2012)
$[C_{12}py][Tf_2N]$	25, 40, 60	0.25 to 10	magnetic suspension balance	Yunus *et al.* (2012)
$[C_4py]$[TfAc]	25, 40, 60	0.25 to 10	magnetic suspension balance	Yunus *et al.* (2012)
$[C_4py]$[DCA]	25, 40, 60	0.25 to 10	magnetic suspension balance	Yunus *et al.* (2012)
[MeBuPy][DCA]	25 to 60	20	gravimetric microbalance	Galán Sánchez (2008)
[MeBuPy][SCN]	25 to 60	20	gravimetric microbalance	Galán Sánchez (2008)
[MeBuPy][$MeSO_4$]	25 to 60	20	gravimetric microbalance	Galán Sánchez (2008)
Phosphonium based ionic liquids				
$[P_{(14)666}]$[Cl]	30	-	lag-time	Ferguson and Scovazzo (2007)
	30	close to atm	surface tension	Kilaru *et al.* (2008)
	20 to 90	1 to 720	high pressure equilibrium cell	Carvalho *et al.* (2010)
	40, 50	80 to 220	isochoric saturation	Manic *et al.* (2012)
	30	1.07 to 1.20	-	Camper *et al.* (2004)

Table 2.6 Literature surveys for the solubility of CO_2 in numerous ionic liquids (cont.)

Ionic liquids	T (°C)	P (bar)	Method	Reference
$[P_{(14)666}][DCA]$	30	-	lag-time	Ferguson and Scovazzo (2007)
	30	close to atm	surface tension	Kilaru *et al.* (2008)
$[P_{(14)666}][Tf_2N]$	30	-	lag-time	Ferguson and Scovazzo (2007)
	30	close to atm	surface tension	Kilaru *et al.* (2008)
	20 to 90	1 to 720	high pressure equilibrium cell	Carvalho *et al.* (2010)
	40, 50	80 to 220	isochoric saturation	Manic *et al.* (2012)
$[P_{2444}][DEP]$	30	-	lag-time	Ferguson and Scovazzo (2007)
	30	close to atm	surface tension	Kilaru *et al.* (2008)
$[P_{(14)444}][DBS]$	30	-	lag-time	Ferguson and Scovazzo (2007)
$[P_{(14)666}][FAP]$	60	-	pressure drop	Blath *et al.* (2011)
Ammonium based ionic liquids				
$[N_{(4)113}][Tf_2N]$	30	close to atm	surface tension	Kilaru *et al.* (2008)
$[N_{(6)113}][Tf_2N]$	30	close to atm	surface tension	Kilaru *et al.* (2008)
$[N_{(10)113}][Tf_2N]$	30	close to atm	surface tension	Kilaru *et al.* (2008)
$[N_{(1)888}][Tf_2N]$	30	close to atm	surface tension	Kilaru *et al.* (2008)
	40, 50	80 to 220	isochoric saturation	Manic *et al.* (2012)
$[N_{(4)111}][Tf_2N]$	30	close to atm	surface tension	Kilaru *et al.* (2008)
	10 to 70	close to atm	isochoric saturation	Jacquemin *et al.* (2007)
	40, 50	80 to 220	isochoric saturation	Manic *et al.* (2012)
	10, 25, 40, 60	up to 13, 13 to 100	gravimetric microbalance, stoichiometric	Muldoon *et al.* (2007)
$[N_{(6)111}][Tf_2N]$	30	close to atm	surface tension	Kilaru *et al.* (2008)

Table 2.6 Literature surveys for the solubility of CO_2 in numerous ionic liquids (cont.)

Ionic liquids	T (°C)	P (bar)	Method	Reference
$[N_{(10)111}][Tf_2N]$	30	close to atm	surface tension	Kilaru *et al.* (2008)
$[N_{(6)222}][Tf_2N]$	30	close to atm	surface tension	Kilaru *et al.* (2008)
$[MeBu_3N][Tf_2N]$	25	13	gravimetric microbalance	Anthony *et al.* (2005)
$[N_{4444}][doc]$	10, 25, 40, 60	up to 13, 13 to 100	gravimetric microbalance, stoichiometric	Muldoon *et al.* (2007)
m-2-HEAA	20 to 80	800	high pressure equilibrium cell	Mattedi *et al.* (2011)
m-2-HEAF	20 to 80	800	high pressure equilibrium cell	Mattedi *et al.* (2011)
HEF	30 to 50	0 to 110	high-pressure cell	Yuan *et al.* (2007)
HEA	30 to 50	0 to 110	high-pressure cell	Yuan *et al.* (2007)
	25, 40, 55	1 to 16	pressure drop	Kurnia *et al.* (2009)
HEL	30 to 50	0 to 110	high-pressure cell	Yuan *et al.* (2007)
	25, 40, 55	1 to 16	pressure drop	Kurnia *et al.* (2009)
THEAA	30 to 50	0 to 110	high-pressure cell	Yuan *et al.* (2007)
THEAL	30 to 50	0 to 110	high-pressure cell	Yuan *et al.* (2007)
HEAF	30 to 50	0 to 110	high-pressure cell	Yuan *et al.* (2007)
HEAA	30 to 50	0 to 110	high-pressure cell	Yuan *et al.* (2007)
HEAL	30 to 50	0 to 110	high-pressure cell	Yuan *et al.* (2007)
BHEAA	25, 40, 55	1 to 16	pressure drop	Kurnia *et al.* (2009)
BHEAL	25, 40, 55	1 to 16	pressure drop	Kurnia *et al.* (2009)
HHEMEA	25, 40, 55	1 to 16	pressure drop	Kurnia *et al.* (2009)
HHEMEL	25, 40, 55	1 to 16	pressure drop	Kurnia *et al.* (2009)

Table 2.6 Literature surveys for the solubility of CO_2 in numerous ionic liquids (cont.)

Ionic liquids	T (°C)	P (bar)	Method	Reference
[choline][Tf_2N]	10, 25, 40, 60	up to 13, 13 to 100	gravimetric microbalance, stoichiometric	Muldoon *et al.* (2007)
Sulfonium based ionic liquids				
[S_{222}][Tf_2N]	60	-	pressure drop	Blath *et al.* (2011)
Piperidinium based ionic liquids				
[MP-piperid][Tf_2N]	60	-	pressure drop	Blath *et al.* (2011)
Pyrrolidinium based ionic liquids				
[MeBuPyrr][Tf_2N]	10, 25	13	gravimetric microbalance	Anthony *et al.* (2005)
[MeBuPyrr][DCA]	25 to 60	20	gravimetric microbalance	Galán Sánchez (2008)
[MeBuPyrr][SCN]	25 to 60	20	gravimetric microbalance	Galán Sánchez (2008)
[MeBuPyrr][TfAc]	25 to 60	20	gravimetric microbalance	Galán Sánchez (2008)
[C_1C_4pyrr][Tf_2N]	30 to 70	close to atm	isochoric saturation	Hong *et al.* (2007)
	40, 50	80 to 220	isochoric saturation	Manic *et al.* (2012)
[bmpyrr][eFAP]	10, 25, 50	18	gravimetric microbalance	Zhang *et al.* (2008)
Guanidium based ionic liquids				
TMGL	24 to 55	0 to 110	high-pressure cell	Zhang *et al.* (2005)

Among the gas solubility measurement methods mentioned before, gravimetric is the most widely used and more accurate method (Soriano *et al.*, 2009b). Soriano *et al.* (2009b) reported the solubility data for CO_2 in three ionic liquids namely: 1-butyl-3-methylimidazolium trifluoromethanesulfonate ([bmim][triflate]), 1-ethyl-3-methylimidazolium ethylsulfate ([emim][$EtSO_4$]), and 1-ethyl-3-methylimidazolium dicyanamide ([emim][C_2N_3]) for temperature ranging from 303.2 K to 343.2 K (30-70 °C) and pressure up to 6.5 MPa (65 bar) by using thermogravimetric microbalance. Among the ionic liquids studied, [bmim][triflate] was observed to have the highest CO_2 solubility. Galán Sánchez (2008) experimentally measured the solubility of CO_2, CH_4, C_2H_4 and C_2H_6 into different cations (imidazolium, pyridinium and pyrrolinium) and anions (tetrafluoroborate ([BF_4^-]), hexafluorophosphate ([PF_6^-]), dicyanamide ([DCA^-]), thiocyanate ([SCN^-]), methylsulfate ([$MeSO_4^-$]), bis(trifluoromethylsulfonyl)imide ([Tf_2N^-]) and trifluoroacetate ([TFA^-])) using a static method with a gravimetric balance IGA-003 at pressures lower than 20 bar and at temperatures between 298 K and 333 K (25-60 °C). It was shown that CO_2 exhibited the highest gas solubility combined with a good selectivity of all studied gases. During the past seven years, Shiflett *et al.* has performed CO_2 absorption measurements in many potential ionic liquids with a gravimetric microbalance IGA-003 under 2 MPa (20 bar) and correlated the experimental CO_2 solubility data using a simple cubic equation of state (EoS). First, the CO_2 solubility in 1-butyl-3-methylimidazolium hexafluorophosphate ([bmim][PF_6]), and 1-butyl-3-methylimidazolium tetrafluoroborate ([bmim][BF_4]) were measured at temperatures of 283.15, 298.15, 323.15, and 348.15 K (10, 25, 50 and 75 °C) (Shiflett and Yokozeki, 2005). Later, Shiflett and Yokozeki (2007) determined the CO_2 solubility in 1-hexyl-3-methyl imidazolium bis(trifluoromethylsulfonyl)imide ([hmim][Tf_2N]) at temperatures of about 282, 297, 323, and 348 K (9, 24, 50 and 75 °C). As reviewed, the gas solubility, especially CO_2, in conventional ionic liquids containing the imidazolium cation have mostly been found in many articles so far. In terms of CO_2 absorption, conventional ionic liquids can absorb and separate CO_2 effectively to a certain extent due to physical absorption mechanism. The CO_2 absorption of these conventional salts, which is far

below that of traditional alkanolamine solutions, is an important drawback even in the fluorinated salts (Zhao *et al.*, 2012). After the high solubility of CO_2 in 1-butyl-3-methylimidazolium acetate ([bmim][Ac]) was known, Shiflett *et al.* (2008) examined the CO_2 solubility in [bmim][Ac] at four isotherms of 283, 298, 323, and 348 K (10, 25, 50 and 75 °C). They obviously found an extremely unusual behavior that [bmim][Ac] could strongly chemically absorb CO_2 at high concentrations up to about 20 mole % of CO_2 with almost no vapor pressure above the mixtures. The result suggested that CO_2 evidently formed a reversible non-volatile molecular complex with [bmim][Ac]. After that, 1-ethyl-3-methylimidazolium acetate ([emim][Ac]), 1-ethyl-3-methylimidazolium trifluoroacetate ([emim][TFA]), and a mixture containing a fixed mole ratio of 49.98 [emim][Ac]/50.02 [emim][TFA] at three temperatures of 298.1, 323.1, and 348.1 K (25, 50 and 75 °C) were investigated. They reported that [emim][Ac] also exhibited strong chemical CO_2 absorption, which had the phase behavior similar to [bmim][Ac]. However, [emim][TFA] did not show the same behavior and physically absorbed CO_2 due to the replacement of the acetate anion methyl group ($CH_3^-COO^-$) with a fluorinated methyl group ($CF_3^-COO^-$), resulting in the significant reduction of high CO_2 solubility. Further explanation was that the electron density could be withdrawn by the CF_3 group, decreasing the Lewis basicity of the anion and consequently reducing the chemical complex formation and CO_2 solubility (Shiflett and Yokozeki, 2009). Recently, vapor-liquid equilibria of CO_2 in 1-ethyl-3-ethylimidazolium acetate ([eeim][Ac]) was examined at four temperatures of 283, 298, 323, and 348 K (10, 25, 50 and 75 °C). The result indicated the formation of a molecular complex with [eeim][Ac], which was similar to [bmim][Ac] and [emim][Ac], and identified the structure of the molecular complex of CO_2 and [eeim][Ac] to be [eeim]-2-carboxylate (Shiflett *et al.*, 2012). Besides the research of Shiflett *et al.* on chemically-absorbing ionic liquids, Maginn (2005b) reported the solubility of CO_2 in 1-butyl-3-methylimidazolium acetate ([bmim][acetate]) in terms of Henry's law constant at temperatures of 25 and 60 °C. The acetate anion showed very low Henry's law constant due to chemical complex. NMR results indicated that the acetate anion extracted a proton from the C_2 position of the imidazolium ring to form acetic acid as proposed in Figure 2.19.

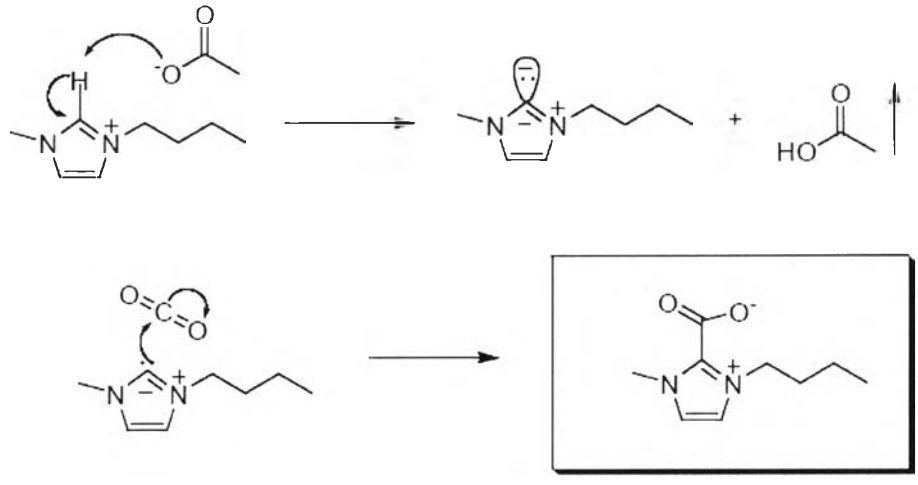

Figure 2.19 Proposed mechanism for enhanced CO_2 solubility in imidazolium acetate (Maginn, 2005b).

Apart from the commonly used imidazolium cations, ionic liquids with hydroxylammonium cations have been gaining interest by many researchers as well. Yuan *et al.* (2007) determined the solubility of CO_2 in eight hydroxylammonium ionic liquids, namely, 2-hydroxyethylammonium formate (HEF), 2-hydroxyethylammonium acetate (HEA), 2-hydroxy ethylammonium lactate (HEL), tri-(2-hydroxy ethyl)-ammonium acetate (THEAA), tri-(2-hydroxy ethyl)-ammonium lactate (THEAL), 2-(2-hydroxy ethoxy)-ammonium formate (HEAF), 2-(2-hydroxy ethoxy)-ammonium acetate (HEAA) and 2-(2-hydroxy ethoxy)-ammonium lactate (HEAL) at the temperatures ranging from 303 to 323K (30-50 °C) and the pressures ranging from 0 to 11 MPa (0-110 bar). The comparison presented that the solubility of CO_2 in these hydroxyl ammonium ionic liquids was in this sequence: THEAL > HEAA > HEA > HEF > HEAL > THEAA ≈ HEL > HEAF. Kurnia *et al.* (2009) reported CO_2 solubility in six hydroxyl ammonium ionic liquids, 2-hydroxyethanaminium acetate (hea), bis(2-hydroxyethyl)ammonium acetate (bheaa), 2-hydroxy-N-(2-hydroxyethyl)-N-methylethanaminium acetate (hhemea), 2-hydroxyethanaminium lactate (hel), bis(2-hydroxyethyl)ammonium lactate (bheal), 2-hydroxy-N-(2-hydroxyethyl)-N-methylethanaminium lactate (hhemel) at temperatures of 298.15, 313.15, and 328.16 K (25, 40 and 55 °C) and pressures

ranging from 100 to 1600 kPa (1-16 bar) using pressure drop method. The CO_2 solubility was arranged in the following order: [hea] > [bheaa] > [hel] > [bheal] > [hhemel] > [hhemea]. The enthalpy and entropy of CO_2 absorption were also investigated and both results exhibited negative values, indicating stronger CO_2 interaction and higher ordering degree of CO_2 dissolution, respectively. Recently, Mattedi *et al.* (2011) studied on the high pressure solubility in N-methyl-2-hydroxyethylammonium formate (m-2-HEAF) and N-methyl-2-hydroxyethyl ammonium acetate (m-2-HEAA) at temperatures from 293 to 353 K (20-80 °C) and pressures up to 80 MPa (800 bar) using a high pressure equilibrium cell. It also could be concluded that ionic liquids comprising the formate presented no specific interaction towards CO_2, whereas those comprising the acetate exhibited the chemical CO_2-IL interaction at low CO_2 mole fractions. Aparicio *et al.* (2011) reported a computational study using quantum chemistry and molecular dynamics methods to analyze CO_2 absorption in two hydroxylammonium ionic liquids, 2-hydroxyethyl-trimethylammonium L-(+)-lactate ([HE3MA]LAC) and tris(2-hydroxyethyl)methylammonium methylsulfate ([3HEMA]MS). The COSMO-RS method was used as a thermodynamic model to predict Henry's law constant as a function of temperature. The predicted Henry's law constant at 298.15 K (25 °C) are 7.5 and 16.2 MPa (75 and 162 bar) for [HE3MA]LAC and [3HEMA]MS, respectively, indicating higher CO_2 solubility in [HE3MA]LAC than in [3HEMA]MS. Even though the hydroxylammonium-based ionic liquids exhibit moderate CO_2 absorption ability due to the presence of hydroxyl groups in the cation, they show more favorably economical and environmental properties than other types of ionic liquids.

2.6.1 Effect of Pressure and Temperature on CO_2 Solubility

It has been established that the solubility of CO_2 increases with an increase in pressure and decreases with an increase in temperature (Zhang *et al.*, 2011). These could be confirmed by the CO_2 solubility data of Anthony *et al.* (2002) in [bmim][PF_6] at three temperatures of 283.15, 298.15, and 273.15 K (10, 25 and 50 °C) and pressures up to 13 bar. As observed in Figure 2.20, the solubility decreased

with an increase in temperature and these curves exhibited a nonlinear trend as the CO_2 pressure was increased. The curves started to flatten out, suggesting that the ionic liquid was beginning to reach its maximum capacity for CO_2.

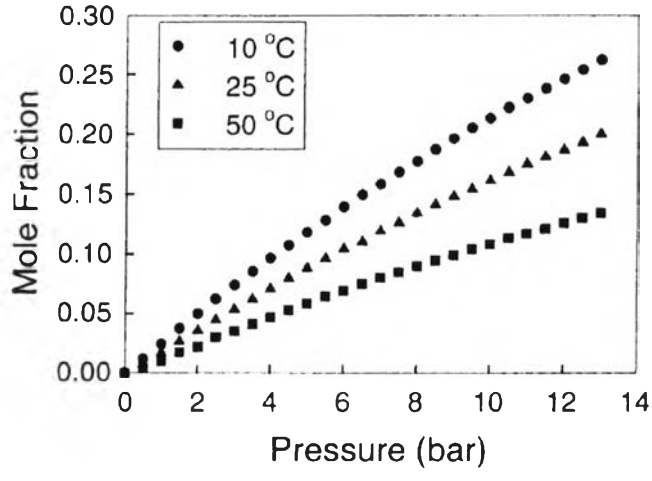

Figure 2.20 CO_2 solubility in [bmim][PF_6] at 283.15, 298.15, and 273.15 K (10, 25 and 50 °C) (Anthony *et al.*, 2002).

The effect of temperature and pressure could also be noticed from the determination of CO_2 solubility by Yunus *et al.* (2012). They examined the solubility of CO_2 in six pyridinium-based ionic liquids, namely, 1-butylpyridinium, bis(trifluoro -methylsulfonyl)imide ([C_4py][Tf_2N]), 1-octylpyridinium bis(trifluoromethyl sulfonyl) imide ([C_8py][Tf_2N]), 1-decylpyridinium, bis(trifluoro-methylsulfonyl)imide ([C_{10}py][Tf_2N]), 1-dodecylpyridinium, bis(trifluoro-methylsulfonyl)imide ([C_{12}py][Tf_2N]), 1-butylpyridinium trifluoroacetate ([C_4py][TfAc]), and 1-butylpyridinium dicyanamide ([C_4py][Dca]) at temperatures of 298.15 K, 313.15 K and 333.15 K (25, 40 and 60 °C) and in the pressure range from 0.25 to 10 bar by using a magnetic suspension balance (MSB). Figure 2.21 shows that the CO_2 solubility linearly increased as pressure increased at low pressures up to 10 bar but exhibited a nonlinear trend at higher pressures. As expected for the effect of temperature, the CO_2 absorption in ionic liquids decreased with an increase in temperature as depicted in Figure 2.22.

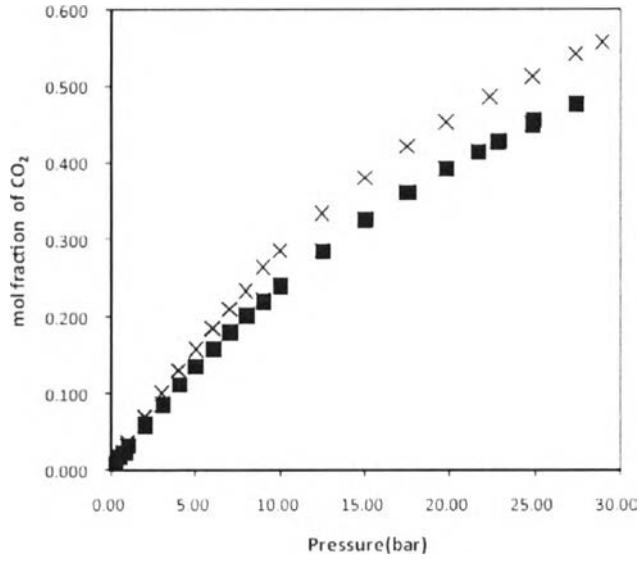

Figure 2.21 The CO_2 solubility as a function of pressure up to 28.98 bar in ■ [C_4py][Tf_2N], and ×[C_{12}py][Tf_2N] at 298.15 K (Yunus *et al.*, 2012).

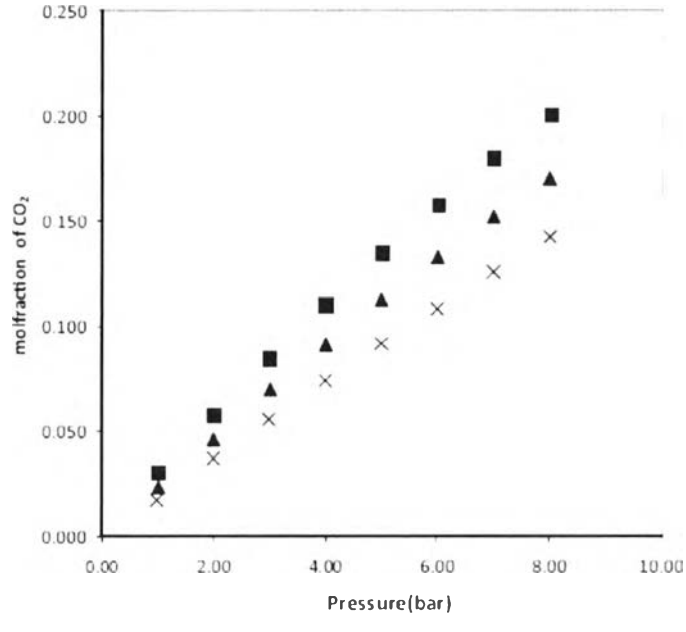

Figure 2.22 The CO_2 solubility in [C_4py][Tf_2N] at: ■ 298.15 K (25 °C), ▲ 313.15 K (40 °C) and × 333.15 K (60 °C) (Yunus *et al.*, 2012).

2.6.2 Effect of Structural Variation on CO_2 Solubility

2.6.2.1 Anion Effect

Maginn (2004) synthesized and acquired nine ionic liquids including 1-n-butyl-3-methylimidazolium acetate, 1-n-butyl-3-methylimidazolium trifluoroacetate, 1-n-hexyl-3-methylimidazolium bis[(trifluoromethyl)sulfonyl]imide, 1-n-hexyl-3-methylimidazolium tris(pentafluoroethyl)trifluorophosphate, 1-butyl-3-methyl imidazolium 2-(2-methoxyethoxy)ethylsulfate, Tetrabutylammonium bis(2-ethylhexyl) sulfosuccinate, 1-methyl-3-(nonafluorohexyl)-imidazolium bis[(trifluoromethyl)sulfonyl]imide, 1-methyl-3-tetreadecylfluorooctylimidazolium bis[(trifluoromethyl)sulfonyl]imide, and 1-n-butyl-3-methylimidazolium perfluoroctonate. The solubilities of CO_2, N_2, O_2, NO, NO_2, N_2O and SO_2 were measured between 283.15 and 343.15 K (10 and 70 °C) using a gravimetric microbalance. The simulation result could explain that the bis[(trifluoromethyl)sulfonyl]imide (Tf_2N^-) presented higher CO_2 solubility than small anions such as the tetrafluoroborate (BF_4^-). Cadena *et al.* (2004) conducted the experimental and molecular modeling studies for the solubility of CO_2 in six different imidazolium-based ionic liquids, 1-butyl-3-methylimidazolium hexafluorophosphate ([bmim][PF_6]), 1-butyl-2,3- dimethylimidazolium hexafluorophosphate ([bmmim][PF_6]), 1-butyl-3-methylimidazolium tetrafluoroborate ([bmim][BF_4]), 1-butyl-2,3-dimethylimidazolium tetrafluoroborate ([bmmim][BF_4]), 1-ethyl-3-methylimidazolium bis(trifluoromethylsulfonyl)imide ([emim][Tf_2N]) and 1-ethyl-2,3-dimethylimidazolium bis(trifluoromethylsulfonyl)-imide ([emmim][Tf_2N]). The CO_2 absorption isotherms were reported at temperatures of 283.15, 298.15, and 273.15 K (10, 25 and 50 °C) and pressures up to approximately 13 bar. They concluded that the anion had the greatest impact on the solubility of CO_2 and the cation played a secondary role. Moreover, it was experimentally observed that the bis(trifluoromethylsulfonyl)imide anion ([Tf_2N^-]) had the highest affinity for CO_2, whereas the tetrafluoroborate anion ([BF_4^-]) or hexafluorophosphate anion ([PF_6^-]) had little difference in CO_2 solubility. Later, Galán Sánchez (2008) studied that the anion had a profound impact on CO_2 solubility in ionic liquids due to the strength of the interaction between CO_2 and anions. It could be summarized that the anion modifications that enhance CO_2 solubility

(decrease Henry's law constant) included the presence of fluorine-containing anions, longer alkyl chain length, and the presence of ether group (Sumon and Henni, 2011). Maginn (2005b) determined the solubility of CO_2 in 1-propyl-3-methylimidazolium tris(heptafluoropropyl)trifluorophposphate ([pmim][bFAP]) at temperatures of 298.15 and 333.15 K (25 and 60 °C) and reported very high CO_2 solubility (very low Henry's law constant) in the highly fluorinated "FAP" anions among physical absorbents. Blath *et al.* (2011) selected ionic liquids with different kinds of cations and anions. The result showed that Henry's law constants for different anions could be arranged by the following order: $[FAP^-] < [Tf_2N^-] \approx [B(CN)_4^-] < [CF_3SO_3^-] < [BF_4^-]$, meaning that more CO_2 solubility in ionic liquids containing $[FAP^-]$ could be observed as presented in Figure 2.23. Sistla *et al.* (2012) employed Hildebrand solubility parameter (δ) to screen ionic liquids by molecular dynamic simulations and they found that an increase in the anion fluorination decreased the δ value in the following order: $[CF_3COO^-] > [Tf_2N^-] > [mFAP^-] > [eFAP^-] > [pFAP^-] > [bFAP^-]$. That means the δ value of the $[bFAP^-]$ anion was closer to that of CO_2, demonstrating high CO_2 solubility in $[bFAP^-]$ anion-based ionic liquids. Based on the effect of anion, it could be concluded that the solubility in the ionic liquids with fluorinated anions is higher than the non-fluorinated anion ones.

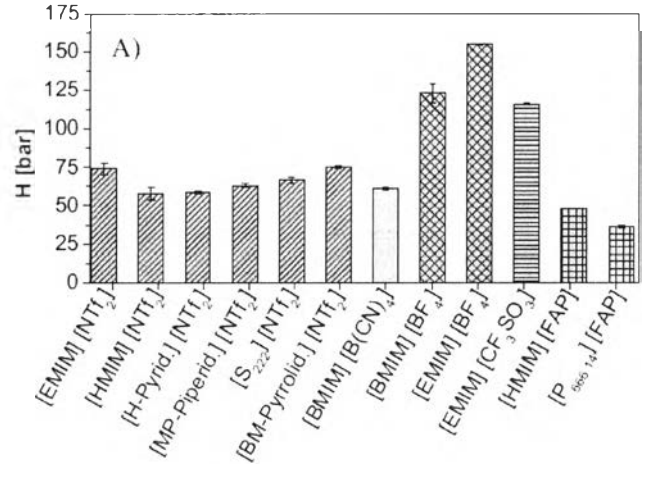

Figure 2.23 Henry's law constants for CO_2 in various ionic liquids at 333.15 K (60 °C) (Blath *et al.*, 2011).

2.6.2.2 Cation Effect

On the other hand, trends to enhance CO_2 solubility (decrease Henry's law constant) due to structural variations relevant to the cation consist of an increase in the alkyl chain length of cation, the alkylation of ammonium and phosphonium cation, the change in cation family, and the substitution of methyl group in C_2 position (Sumon and Henni, 2011). The effect of alkyl chain length was also investigated by Blath *et al.* (2011). As the alkyl chain length on cations increased, the lower Henry's law constant could be obtained, resulting in higher CO_2 solubility. More interestingly, they found that the presence of phosphonium cation was likely to have smaller Henry's law constant, thus higher CO_2 solubility. Yunus *et al.* (2012) studied on the effect of alkyl chain length of pyridinium-based ionic liquids, $[C_4py][Tf_2N]$, $[C_8py][Tf_2N]$, $[C_{10}py][Tf_2N]$ and $[C_{12}py][Tf_2N]$, and described that the CO_2 absorption marginally increased with an increase in the alkyl chain length as illustrated in Figure 2.24. Furthermore, they observed that changing the cation type from imidazolium- to pyridinium- based ionic liquids with the same anion had no difference in the CO_2 solubility.

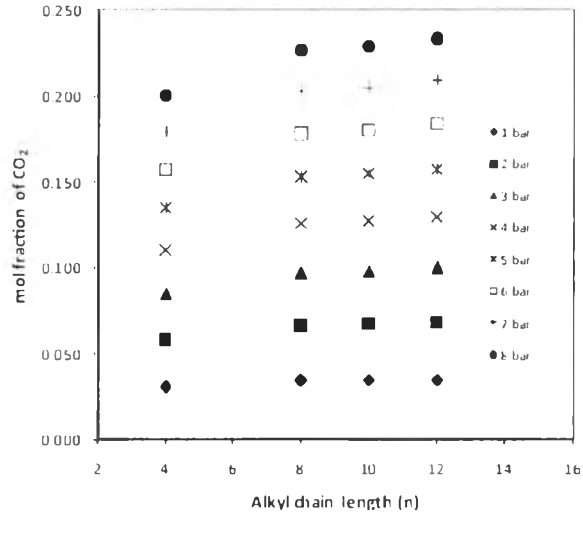

Figure 2.24 The effect of alkyl chain length of cations on the CO_2 solubility in $[C_4py][Tf_2N]$, $[C_8py][Tf_2N]$, $[C_{10}py][Tf_2N]$ and $[C_{12}py][Tf_2N]$ at 298.15 K (25 °C) (Yunus *et al.*, 2012).

2.7 Thermodynamic Modeling

In recent years, several different theoretical approaches, correlations and equations of state (EoS) have been used to attain accurate models for the appropriate description of thermodynamic properties of ionic liquids. Classical cubic equations, activity coefficient and group contribution methods, quantum chemistry calculations and statistical mechanics based molecular approaches are the models which have been applied to describe the thermodynamic behavior and characteristic of ionic liquids and the solubility of gases in them (Vega *et al.*, 2010). It has been reported that several works performed the estimation of the critical properties of ionic liquids by group contribution methods and used simple cubic equations of state to explain the phase behavior of CO_2 in ionic liquids (Shin and Lee, 2008; Song *et al.*, 2009; Yim *et al.*, 2011). In this section, a group contribution method for critical property estimation, equations of state and an activity coefficient model used in this work will be explained in more detail.

2.7.1 Group Contribution Methods for Critical Properties

The knowledge regarding the critical properties and other physical parameters is necessarily used to develop thermodynamic models for pure components and mixtures. For ionic liquids and mixtures comprising ionic liquids, the critical properties cannot be experimentally measured since most of the ionic liquids start to decompose when the temperature approaches the normal boiling point, but such properties are still required to correlate experimental data in thermodynamic modeling. The common method to estimate the critical properties for many substances is the so-called group contribution methods, which are used when the critical properties are not available. Several group contribution methods were proposed in the literature. Apparently, a "modified Lydersen-Joback-Reid" method proposed by Valderrama and Robles (2007), which combined the best results of Lydersen method with the best results of Joback-Reid method, gave good results for molecules having high molecular weight. This approach considered the equations of Lydersen for the critical pressure and the critical volume, while the equations of Joback-Reid for the normal boiling temperature and the critical temperature. The

modified Lydersen-Joback-Reid method is summarized in the following four equations:

$$T_b = 198.2 + \sum n\Delta T_{bM} \tag{2.4}$$

$$T_c = \frac{T_b}{A_M + B_M \sum n\Delta T_M - (\sum n\Delta T_M)^2} \tag{2.5}$$

$$P_c = \frac{M}{[C_M + \sum n\Delta P_M]^2} \tag{2.6}$$

$$V_c = E_M + \sum n\Delta V_M \tag{2.7}$$

In these equations, n is the number of times that a group appears in the molecule, T_b is the normal boiling temperature, ΔT_{bM} is the contribution to the normal boiling temperature, T_c is the critical temperature, ΔT_M is the contribution to the critical temperature, P_c is the critical pressure, ΔP_M is the contribution to the critical pressure, V_c is the critical volume, ΔV_M is the contribution to the critical volume, M is the molecular mass, and A_M, B_M, C_M, and E_M are constants. The values of these constants are A_M = 0.5703, B_M = 1.0121, C_M = 0.2573, and E_M = 6.75. The values of the contributions to T_b, T_c, P_c, and V_c are summarized in Table 2.7.

Since no experimental critical properties were available to evaluate the accuracy of the estimated values, the liquid densities of the ionic liquids are determined as a consistency test for the predicted properties using a generalized correlation based on the equation of Spencer and Danner (Spencer and Danner, 1972), which requires only the normal boiling temperature, the molecular weight, and the critical properties:

$$\rho_L = \frac{MP_c}{RT_c}\left[\frac{0.3445P_cV_c^{1.0135}}{RT_c}\right]^{\Omega} \tag{2.8}$$

$$\Omega = -\left[\frac{1 + (1 - T_R)^{2/7}}{1 + (1 - T_{bR})^{2/7}}\right] \tag{2.9}$$

In these equations, ρ_L is the liquid density (g/cm^3), R is the universal ideal gas constant, T_R is the reduced temperature ($T_R = T/T_c$), and T_{bR} is the reduced temperature at the normal boiling point ($T_{bR} = T_b/T_c$).

Table 2.7 Groups considered for the Modified Lydersen-Joback-Reid method and equations describing the model (Valderrama *et al.*, 2008)

Groups	ΔT_{bM}	ΔT_M	ΔP_M	ΔV_M
without rings				
$-CH_3$	23.58	0.0275	0.3031	66.81
$-CH_2-$	22.88	0.0159	0.2165	57.11
>CH-	21.74	0.0002	0.1140	45.70
>C< [>C-]*	18.18	-0.0206	0.0539	21.78
$=CH_2$	24.96	0.0170	0.2493	60.37
=CH-	18.25	0.0182	0.1866	49.92
=C<	24.14	-0.0003	0.0832	34.90
-O- [-O]*	22.42	0.0051	0.1300	15.61
>C=O	94.97	0.0247	0.2341	69.76
-COO-	81.10	0.0377	0.4139	84.76
>N- [>N<]*	11.74	-0.0028	0.0304	26.70
-N=	74.60	0.0172	0.1541	45.54
-CN	125.66	0.0506	0.3697	89.32
-F [F]	-0.03	0.0228	0.2912	31.47
-Cl [Cl]	38.13	0.0188	0.3738	62.08
-I [I]	93.84	0.0148	0.9174	100.79
with rings				
$-CH_2-$	27.15	0.0116	0.1982	51.64
=CH-	26.73	0.0114	0.1693	42.55
>C<	21.32	-0.0180	0.0139	17.62
=C<	31.01	0.0051	0.0955	31.28
>N- [>N<]*	68.16	0.0063	0.0538	25.17
-N= [>N=]*	57.55	-0.0011	0.0559	42.15
New groups				
-B	-24.56	-0.0264	0.0348	22.45
-P	34.86	0.0067	0.1776	67.01
-S- [>S-]*	117.52	-0.0004	0.6901	184.67
$-SO_2-$	147.24	-0.0563	-0.0606	112.19
Model equations				Constants
$T_b = 198.2 + \sum n\Delta T_{bM}$ $T_c = \frac{T_b}{\left[A_M - B_M \sum n\Delta T_M - \left(\sum n\Delta T_M\right)^2\right]}$		$P_c = \frac{M}{\left[C_M - \sum n\Delta P_M\right]^2}$ $V_c = E_M - \sum n\Delta V_M$		$A_M = 0.5703$ $B_M = 1.0121$ $C_M = 0.2573$ $E_M = 6.75$

Not only the critical properties but also the acentric factors (ω) of the ionic liquids are required in order to calculate the parameters of the equation of state. The acentric factor is calculated by the following expression derived from the definition of this property:

$$\omega = \frac{(T_b - 43)(T_c - 43)}{(T_c - T_b)(0.7T_c - 43)} log\left[\frac{P_c}{P_b}\right] - \frac{(T_c - 43)}{(T_c - T_b)} log\left[\frac{P_c}{P_b}\right] + log\left[\frac{P_c}{P_b}\right] - 1 \quad (2.10)$$

In this equation, the calculated critical properties and the calculated normal boiling temperature are needed. The normal boiling temperature is considered at the normal boiling pressure (P_b = 1.01325 bar).

Valderrama and Robles (2007) determined the critical properties (T_c, P_c, V_c), the normal boiling temperatures (T_b), and the acentric factors (ω) of 50 ionic liquids using an extended group contribution methods based on the well-known concepts of Lydersen and of Joback and Reid. As for the accuracy and consistency of the estimated values, the liquid density calculation was performed to test the estimates whether or not they were acceptable. The results showed that the calculated critical properties, normal boiling temperatures, and acentric factors were sufficiently acceptable for engineering calculations, for generalized correlations, and for equation of state methods with the average deviation and the average absolute deviation of 1.6 and 5.2%, respectively. Valderrama *et al.* (2008) further determined these properties for 200 ionic liquids and summarized some statistical values, such as the average, absolute, and maximum deviations observed between predicted and experimental densities. The overall deviations were found to be less than -0.4% and the overall absolute deviations were less than 5.9%, whereas only 36 of the 200 ionic liquids presented deviations greater than 10%.

2.7.2 Equations of State (EoS)

Numerous industrial applications require knowledge of the phase equilibria of mixtures. The phase equilibria can be predicted from a proper thermodynamic model. Such models are necessary to correlate existing experimental data and to predict phase equilibria in regions where experimental data are not available. An equation of state is a thermodynamic equation describing the state of

matter under a given set of physical conditions. The equation provides a mathematical relationship between two or more state functions associated with the matter such as pressure, volume and temperature. In general, cubic equations of state give pressure in terms of volume and temperature of a substance are the most commonly used models to predict phase equilibria. Several equations of state have been proposed such as the van der Waals equation, the Redlich-Kwong (RK) equation, the Soave-Redlich-Kwong (SRK) equation, and the Peng-Robinson (PR) equation. Of all equations, the van der Waals equation is the most important since this model provides a basis for the rest of the equations of state. All cubic equations of state contain two constants which are an attractive parameter (a) and a repulsion parameter (b). Hence, they are named two-constant equations of state. The latter parameter involving repulsion also refers to the co-volume parameter which is sometimes called the effective molecular volume. Computation by the cubic equations of state with a relevant mixing rule can yield reasonable predictions for vapor-liquid equilibrium of fluids (Walas, 1985; Sandler, 1999; Mushrif, 2004). With respect to multicomponent mixture, binary interaction parameters in the mixing rules, which take into account the difference in the interaction of unlike molecules, were optimized from phase-equilibrium data regression, such as VLE data. In general, the interaction parameters have some kind of temperature dependency. The dependency of temperature is usually a linear function, although in some cases polynomials could also be used.

One of the main advantages of using the equations of state is that they are straightforward to use and they are present in any process simulator. In most cases, several parameters including temperature, pressure, and composition are required for ionic liquids' calculations. However, the equations of state are missing some important parts of the physical nature of ionic liquids. For example, the cations and anions of ionic liquids are considered as a neutral pair, but they still exhibit the presence of polarity and hydrogen bonding ability. Nevertheless, the equations of state do not take these two facts into account. Moreover, the equations of state present a major drawback since they require critical parameters of the ionic liquids which can only be obtained indirectly and with large uncertainties. These equations can be used for correlation purposes but the predictive ability is limited by this fact

(Vega *et al.*, 2010). This section will provide and discuss sets of equations for the standard Redlich-Kwong-Soave (SRK-EoS), the standard Peng-Robinson (PR-EoS), and the Redlich-Kwong-Aspen equations of state (The SRK with quadratic mixing rules), which are available in the AspenPlus simulator.

2.7.2.1 The Standard Redlich-Kwong-Soave (SRK-EoS)

Redlich and Kwong (1949) proposed an equation of state comprising two individual coefficients, which enhances results satisfactorily (Redlich and Kwong, 1949). Afterwards, Soave (1972) proposed the modified Redlich-Kwong equation by presuming the parameter a in the original equation to be temperature-dependent. A generalized correlation for the modified parameter can be derived by introducing an acentric factor as a third parameter (Soave, 1972). In AspenPlus, the SRK-EoS is recommended for hydrocarbon processing applications such as gas processing, refinery, and petrochemical processes. The original Redlich-Kwong (RK) equation of state is:

$$P = \frac{RT}{V-b} - \frac{a/T^{0.5}}{V(V+b)} \tag{2.11}$$

This equation was developed by replacing the term $a/T^{0.5}$ with a more general dependent term a(T):

$$P = \frac{RT}{V-b} - \frac{a(T)}{V(V+b)} \tag{2.12}$$

The pure components parameters for SRK-EoS are calculated as:

$$a_i = \alpha_i 0.42747 \frac{R^2 T_{ci}^2}{P_{ci}} \tag{2.13}$$

$$b_i = 0.08664 \frac{RT_{ci}}{P_{ci}} \tag{2.14}$$

These expressions are derived by applying the critical constraint to the equation of state under these conditions:

$$\alpha_i(T_{ci}) = 1.0 \tag{2.15}$$

The parameter α_i is a temperature function introduced by Soave (1972) in the RK-EoS to enhance the correlation of the component vapor pressure:

$$\alpha_i(T) = \left[1 + m_i\left(1 - T_{ri}^{0.5}\right)\right]^2 \tag{2.16}$$

The parameter m_i is expressed in the form of the correlation with the acentric factor:

$$m_i = 0.48508 + 1.55171\omega_i - 0.15613\omega_i^2 \tag{2.17}$$

Equations 2.13-2.17 are the standard Soave-Redlich-Kwong (SRK) formulations.

The mixing parameters for the standard SRK-EoS are defined by the mixing rules that are most commonly used:

$$a = \sum_i \sum_j x_i x_j a_{ij} \tag{2.18}$$

$$a_{ij} = \left(a_i a_j\right)^{0.5}\left(1 - k_{ij}\right) \tag{2.19}$$

$$b = \sum_i x_i b_i \tag{2.20}$$

In these equations, k_{ij} is a binary interaction parameter, where $k_{ij} = k_{ji}$. For the standard SRK-EoS, k_{ij} is temperature dependency as observed from the following equation:

$$k_{ij} = k_{ij}^1 + k_{ij}^2 T + k_{ij}^3 / T \tag{2.21}$$

Usually, a linear function of k_{ij} depending on temperature will be taken into account.

2.7.2.2 The Standard Peng-Robinson (PR-EoS)

Peng and Robinson (1976) developed the equation of state in which the attractive pressure term of the semiempirical van der Waals equation has been modified. In AspenPlus, the standard Peng-Robinson equation of state is the original formulation of the Peng-Robinson equation of state with the standard alpha function. It is also recommended for hydrocarbon processing applications such as gas processing, refinery, and petrochemical processes. The results of the standard Peng-Robinson equation are comparable to those of the standard Redlich-Kwong-Soave equation. The standard Peng-Ronbinson equation of state (PR-EoS) is proposed as follows:

$$P = \frac{RT}{V - b} - \frac{a(T)}{V(V + b) + b(V - b)} \tag{2.22}$$

The pure component parameters for the PR-EoS are calculated as:

$$a_i = \alpha_i 0.45724 \frac{R^2 T_{ci}^2}{P_{ci}} \tag{2.23}$$

$$b_i = 0.07780 \frac{RT_{ci}}{P_{ci}} \tag{2.24}$$

These expressions are derived by applying the critical constraints to the equation of state under these conditions:

$$\alpha_i(T_{ci}) = 1.0 \tag{2.25}$$

The parameter α_i is a function of temperature. It was originally introduced by Soave (1972) in the RK-EoS . This parameter improves the correlation of the pure component vapor pressure. The relationship between α_i and T_r can be linearized by the following equation which is similar to that obtained by Soave (1972):

$$\alpha_i(T) = \left[1 + m_i\left(1 - T_{ri}^{0.5}\right)\right]^2 \tag{2.26}$$

The parameter m_i can be correlated against the acentric factor:

$$m_i = 0.37464 + 1.54226\omega_i - 0.26992\omega_i^2 \tag{2.27}$$

Equations 2.23-2.27 are the standard Peng-Robinson (PR) formulations.

The mixing parameters for the standard PR-EoS are defined by the mixing rules that are most commonly used:

$$a = \sum_i \sum_j x_i x_j a_{ij} \tag{2.28}$$

$$a_{ij} = \left(a_i a_j\right)^{0.5}\left(1 - k_{ij}\right) \tag{2.29}$$

$$b = \sum_i x_i b_i \tag{2.30}$$

In these equations, k_{ij} is a binary interaction parameter, where $k_{ij} = k_{ji}$. For the standard PR-EoS, k_{ij} is temperature dependency as observed from the following equation:

$$k_{ij} = k_{ij}^1 + k_{ij}^2 T + k_{ij}^3 / T \tag{2.31}$$

Also, a linear function of k_{ij} depending on temperature will be taken into account.

2.7.2.3 The Redlich-Kwong-Aspen (The SRK with Quadratic Mixing Rules)

In AspenPlus, the Redlich-Kwong-Aspen equation of state is the basis for the RK-ASPEN property method. It can be used for hydrocarbon processing applications. It is also used for more polar components and mixtures of hydrocarbons, and for light gases at medium to high pressure. The two-parameter cubic equation of RK-ASPEN is based on a theory of the Soave-Redlich-Kwong (SRK) equation which was derived from the Redlich-Kwong (RK) equation of state (Redlich and Kwong, 1949) and further developed by Soave (1972). The following equation of the SRK-EoS is expressed with a more general temperature-dependent term a(T):

$$P = \frac{RT}{V-b} - \frac{a(T)}{V(V+b)} \tag{2.32}$$

The pure components parameters for SRK-EoS are calculated as:

$$a_i = \alpha_i 0.42747 \frac{R^2 T_{ci}^2}{P_{ci}} \tag{2.33}$$

$$b_i = 0.08664 \frac{RT_{ci}}{P_{ci}} \tag{2.34}$$

These expressions are derived by applying the critical constraint to the equation of state under these conditions:

$$\alpha_i(T_{ci}) = 1.0 \tag{2.35}$$

The parameter α_i is a temperature function introduced by Soave (1972) in the RK-EoS to enhance the correlation of the component vapor pressure:

$$\alpha_i(T) = \left[1 + m_i\left(1 - T_{ri}^{0.5}\right)\right]^2 \tag{2.36}$$

The parameter m_i is expressed in the form of the correlation with the acentric factor:

$$m_i = 0.48508 + 1.55171\omega_i - 0.15613\omega_i^2 \tag{2.37}$$

For multicomponent equilibria, mixing rules and combining rules which relate the properties of the pure components to the properties of the

mixtures are applied. The mixture parameters in liquid phase are calculated from the so-called quadratic mixing rules.

$$a = \sum_i \sum_j x_i x_j a_{ij} \tag{2.38}$$

$$a_{ij} = (a_i a_j)^{0.5}(1 - k_{ij}) \tag{2.39}$$

$$b = \sum_i \sum_j x_i x_j b_{ij} \tag{2.40}$$

$$b_{ij} = \frac{(b_i + b_j)}{2}(1 - l_{ij}) \tag{2.41}$$

In equation 2.40, $b_{ii} = b_i$ and $b_{jj} = b_j$. k_{ij} and l_{ij} in equations 2.39 and 2.41 are binary interaction parameters. In the Redlich-Kwong-Aspen equation of state, the interaction parameters are linearly temperature-dependent:

$$k_{ij} = k_{ij}^0 + k_{ij}^1 \frac{T}{1000} \tag{2.42}$$

$$l_{ij} = l_{ij}^0 + l_{ij}^1 \frac{T}{1000} \tag{2.43}$$

In these equations, parameters k_{ij}^0, k_{ij}^1, l_{ij}^0 and l_{ij}^1 are constant.

2.7.3 Activity Coefficient Model

As a result of the limitations that mentioned previously for the equations of state, several excess Gibbs energy models, such as the Wilson's equation, the Non-Random Two-Liquid (NRTL), and the Universal Quasi-Chemical (UNIQUAC), have been used to describe the systems involving ionic liquids (Vega *et al.*, 2010). In this work, we correlate the CO_2 solubility data using the NRTL equations, which will be expressed in this section.

2.7.3.1 The Non-Random Two-Liquid (NRTL)

The NRTL model is an activity coefficient model that correlates the activity coefficients of a compound with its mole fraction in the liquid phase concerned. In AspenPlus, the NRTL model will calculate the liquid activity coefficients. It is recommended for highly non-ideal chemical systems, and can be

used for VLE and LLE applications. The model for the derivation of the NRTL equation of the excess Gibbs energy is a two-cell theory. The assumption is that the liquid has a structure made up of molecules of type 1 or of type 2 being surrounded proportionally by molecules of both types in a binary mixture, as represented in Figure 2.25. Gibbs energies of interaction between molecules, g_{ij}, are defined, where subscript j refers to the central molecule (Walas, 1985). The concept of NRTL is that the local concentration around a molecule is different from the bulk concentration. This difference is due to a difference between the interaction energy of the central molecule with the molecules of its own kind g_{ii} and that with the molecule of the other kind g_{ij}. The energy difference introduces nonrandomness at the local molecular level.

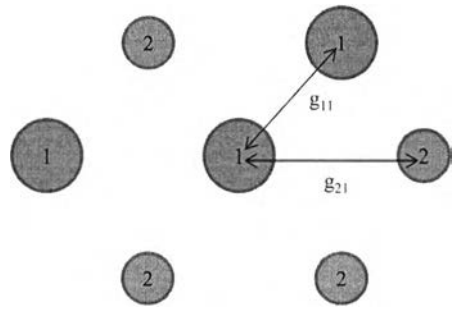

(a). Type 1 molecule at the center of the cluster.

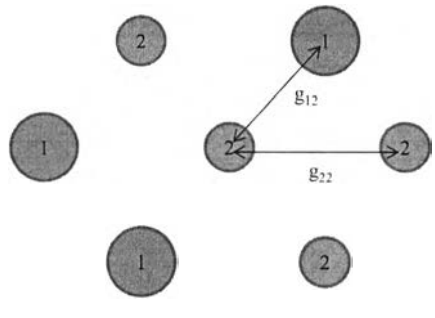

(b). Type 2 molecule at the center of the cluster.

Figure 2.25 Two types of molecular clusters or cells of binary liquid mixtures.

The binary activity coefficients of the NRTL model are given by:

$$ln\gamma_1 = x_2^2\left[\tau_{21}\left(\frac{G_{21}}{x_1 + x_2G_{21}}\right)^2 + \left(\frac{\tau_{12}G_{12}}{(x_2 + x_1G_{12})^2}\right)\right] \tag{2.33}$$

$$ln\gamma_2 = x_1^2\left[\tau_{12}\left(\frac{G_{12}}{x_2 + x_1G_{12}}\right)^2 + \left(\frac{\tau_{21}G_{21}}{(x_1 + x_2G_{21})^2}\right)\right] \tag{2.34}$$

where,

$$G_{12} = \exp(-\propto_{12}\tau_{12}) \tag{2.35}$$

$$G_{21} = \exp(-\propto_{12}\tau_{21}) \tag{2.36}$$

$$\tau_{12} = (g_{12} - g_{22})/RT \tag{2.37}$$

$$\tau_{21} = (g_{21} - g_{11})/RT \tag{2.38}$$

In these equations, the Gibbs energies of the pure substances, g_{12} and g_{21}, are presumed to be equivalent ($g_{12} = g_{21}$). τ_{12}, τ_{21} and α_{12} are three binary parameters adjusted to the experimental solubility data of ionic liquids. In general, τ_{12} and τ_{21} are temperature dependent, while α_{12} is usually set as a constant unique value ($\alpha_{12} = \alpha_{21}$). The parameter α_{12} depends on the chemical nature, which is assumed to be characteristic of the nonrandomness of the mixture. It is typically in a range of 0.2-0.47, but mostly set as a value of 0.3. It was reported that the correlation with $\alpha_{12} = 0.3$ produced more accurate results according to root-mean-square deviation (rmsd) values (Al-Rashed *et al.*, 2012).

2.8 Derivation of Henry's law constant

In 1803, William Henry stated that at a constant temperature, the amount of a given gas that dissolves in a given type and volume of liquid is directly proportional to the partial pressure of that gas in equilibrium with that liquid. An equivalent meaning of this statement is that the solubility of a gas in a liquid is directly proportional to the partial pressure of the gas above the liquid. Henry's law

constant can be defined in several ways. According to Husson-Borg *et al.* (2003), the Henry's law constant is defined as:

$$H_{2,1}(p_2,T) \equiv \lim_{x_2 \to 0} \frac{f_2^L(p_2,T,x_2)}{x_2} \tag{2.39}$$

In this work, we define an ionic liquid as component 1 and CO_2 as component 2. Therefore, $f_2^L(p_2,T,x_2)$ is the fugacity of CO_2 dissolved in the ionic liquid phase, x_2 is the mole fraction of CO_2 in the liquid phase, p_2 is the partial pressure of CO_2, and T is the temperature. At equilibrium, the fugacities of each component in the liquid phase are equal to those in the vapor phase, which can be expressed as:

$$f_2^L(p_2,T,x_2) = f_2^V(p_2,T,y_2) = \emptyset_2(p_2,T,y_2)y_2p_2 \tag{2.40}$$

where $\phi_2(p_2,T,y_2)$ is the fugacity coefficient of CO_2. For the (ionic liquid + CO_2) system, the ionic liquid is considered to have negligible vapor pressure.

$$\emptyset_2(p_2,T,y_2)y_2p_2 = \emptyset_2(p_2,T)p_2 \tag{2.41}$$

For very low concentrations of CO_2 in the ionic liquid, Henry's law constant can be expressed as:

$$H_{2,1}(p_2,T) = \lim_{x_2 \to 0} \frac{f_2^L(p_2,T,x_2)}{x_2} = \lim_{x_2 \to 0} \frac{\emptyset_2(p_2,T)p_2}{x_2} = \lim_{x_2 \to 0} \frac{\emptyset_2(p_2,T)x_2P}{x_2} \tag{2.42}$$

According to Anthony (2004), the Henry's law constant, in general, shows the dependency on temperature. However, it is relatively insensitive to pressure, especially over a range of low pressures. For an ideal system, knowing the fugacity of CO_2 in the ionic liquid phase equivalent to the fugacity of CO_2 in the CO_2 phase is able to approximate the gas phase fugacity as the gas phase pressure. The following form of Henry's law can be obtained:

$$p_2 = H_{2,1}(T) \cdot x_2 \tag{2.43}$$

where $H_{2,1}(T)$ has a unit of pressure and is inversely proportional to the mole fraction of CO_2 in the ionic liquid.

2.9 Derivation of Enthalpies and Entropies of Absorption

In accordance with Anthony (2004), enthalpies and entropies of absorption can be found by taking temperature effect on gas solubilities into consideration. The enthalpy is related to the strength of interaction between the dissolved gas and the liquid, while the entropy demonstrates the level of ordering that takes place in the liquid/gas mixture. These properties can be examined from the following thermodynamic relations:

$$\Delta h_2 = \bar{h}_2 - h_2^{ig} = RT\left(\frac{\partial lnx_2}{\partial lnT}\right)_P \left(\frac{\partial lna_2}{\partial lnx_2}\right)_{P,T} \tag{2.44}$$

$$\Delta s_2 = \bar{s}_2 - s_2^{ig} = R\left(\frac{\partial lnx_2}{\partial lnT}\right)_P \left(\frac{\partial lna_2}{\partial lnx_2}\right)_{P,T} \tag{2.45}$$

where $\bar{h}_2$ and $\bar{s}_2$ are the partial molar enthalpy and entropy of the gas which is CO_2 in the solution of ionic liquid and CO_2, h_2^{ig} and s_2^{ig} are the enthalpy and entropy of the pure CO_2 in the ideal gas phase, and a_1 is the activity of CO_2 in the mixture:

$$a_2 = \gamma_2 \cdot x_2 \tag{2.46}$$

Equations 2.44 and 2.45 are equivalent to

$$\Delta h_2 = R\left(\frac{\partial lnP}{\partial(1/T)}\right)_{x_2} \tag{2.47}$$

$$\Delta s_2 = -R\left(\frac{\partial lnP}{\partial lnT}\right)_{x_2} \tag{2.48}$$

These provide Δh_2 and Δs_2 at a specific mole fraction of CO_2 in the ionic liquid (x_2). In the Henry's law region (i.e. when γ_2 is independent of x_2), the last terms in equations 2.44 and 2.45 are unity, thus being able to reduce to the familiar van't Hoff forms:

$$\Delta h_2 = -R\left(\frac{\partial lnx_2}{\partial(1/T)}\right)_P = R\left(\frac{\partial lnH_{2,1}}{\partial(1/T)}\right)_P \tag{2.49}$$

$$\Delta s_2 = R\left(\frac{\partial ln x_2}{\partial ln T}\right)_P = -R\left(\frac{\partial ln H_{2,1}}{\partial ln T}\right)_P \tag{2.50}$$

Equations 2.49 and 2.50 yield Δh_2 and Δs_2 which are valid at infinite dilution. These equations will also give the same Δh_2 and Δs_2 calculated by equations 2.47 and 2.48 as the x_2 becomes adequately small to be in the infinite dilution range.